EVALUATING THE BIOMASS OF PALATABLE GRASS SPECIES IN THE COMMUNAL RANGELAND USING THE INTEGRATION OF UAV DATA WITH HIGH-RESOLUTION SATELLITE DATA

By

Murendeni Sharon Mavhina
(17011422)

Submitted in fulfilment of the academic requirements for the degree of Master of Science in Ecology and Resource Management

In the

Department of Ecology and Resource Management
School of Environmental Sciences, at the University of Venda

Supervisor: Dr. OE Malahlela
Co-supervisor: Dr. FM Murungweni

March 2025

© University of Venda

University of Venda
Creating Future Leaders

Declaration

I, the undersigned, Murendeni Sharon Mavhina, hereby declare that the work contained in this thesis is my own work, and I hereby submit it for the degree of Master of Ecology and Resource Management at the University of Venda. This work has not been previously submitted by me for a degree at this or any other tertiary institution.



M.S. Mavhina
(Student)

© University of Venda

Acknowledgments

I would like to express my sincere gratitude to God Almighty for giving me the strength, wisdom, and ability to successfully conduct and complete my thesis.

I wish to express gratitude to the following people who have been by my side throughout my academic journey, persevering through the difficulties with me even when there was no hope:

To my beloved family, whose unfailing love, support, and continuous encouragement got me through the hardships faced. Your prayers have been the foundation of my success.

To my Supervisors, Dr. OE Malahlela and Dr. FM Murungweni, without your expertise, guidance, patience, and contribution, this work would not have been completed. Thank you for the motivation, support, and patience, and for making sure I push beyond my limits.

To my Sponsor, South African National Space Agency (SANSA), thank you for making sure that my financial needs were met during my studies. Your contribution has made it possible for me to pursue my academic aspirations. I am grateful for your understanding and patience.

© University of Venda

General Abstract

The biomass of palatable grass species plays a crucial role in sustaining livestock within rural and communal rangelands. Accurate biomass mapping techniques are essential in providing insights into the quantification and distribution of palatable grass biomass. Assessing the distribution of biomass and the effectiveness of biomass mapping is one of the important steps for the provision of crucial information on the health of rangelands while facilitating effective land management and sustainable resource utilisation. This study aimed to evaluate the biomass of palatable grass species in communal rangeland by integrating the use of unmanned aerial vehicle (UAV) obtained in December 2022 data with high-resolution PlanetScope(PS) satellite imagery (3 m spatial resolution) obtained in October 2022. The Supervised Maximum Likelihood Classification (MLC) algorithm was employed in mapping land cover classes across the study and achieved overall accuracy of 99.29% and a kappa of 0.98, indicating high reliability in mapping grazing areas. The grazing area size was quantified as 33 695 hectares (ha) from the total 66 982 hectares (ha) of the study area, with grazing areas accounting for 50%, followed by built-up areas (26%) and water bodies (0.21%). The study also evaluated the performance of linear and non-linear regression models for mapping the Palatable grass biomass by comparing the model performance using remotely sensed data derived from the PS imagery. According to the results, non-linear regression models outperformed the linear models, and obtained a root mean squared error (RMSE), mean absolute error (MAE) and coefficient of determination (R^2) of 2.15, 1.69 and 0.11, respectively. Additionally, the study tested the performance of linear and non-linear models for mapping palatable grass biomass using the unmanned aerial vehicle (UAV) and PlanetScope data. The comparison between the PlanetScope subset data and the UAV data obtained an RMSE of 2.36 , MAE of 3.22 and R^2 of 0.35 for the subset image, and an RMSE, MAE and R^2 of 9.83, 6.57 and 0.23, respectively for the UAV data. Both the satellite imagery and the UAV imagery were used to develop and test models for predicting and mapping palatable grass biomass with the use of integration of spectral bands, vegetation indices, and grey level co-occurrence matrix (GLCM) features. These findings demonstrate possibilities offered by remote sensing techniques in improving rangeland management and sustainable resource planning.

Keywords: Communal grazing areas, linear regression, Maximum Likelihood classification (MLC), non-linear regression, palatable grass biomass, PlanetScope imagery, UAV image.

© University of Venda

List of figures

Figure 1.1: Flowchart of the thesis outline used in the study..... 4
Figure 2.1: The location of the study area with sampling points..... 10
Figure 2.2: Classification map of Vhembe east villages from PlanetScope imagery using Maximum likelihood classifier with five class categories: Water, Vegetation, Built-up areas, Grazing areas and Woodlands..... 15
Figure 2.3: Grazing areas distribution within the study area..... 16
Figure 2.4: Chart depicting land cover classes as per the area size they hold within the study area..... 17
Figure 3.1: Location of the study area and distribution of field survey points for the PlanetScope and UAV site..... 26
Figure 3.2: Comparison of Linear and Non-linear (Exponential) models on PlanetScope data with the use of bands, indices, and GLCM measures as predictor variables as computed from the initial model..... 37
Figure 3.3: Palatable grass biomass spatial map as predicted by the linear regression model derived from the PlanetScope primary image..... 38
Figure 3.4: Scatterplot of the measured vs predicted palatable grass biomass, (g/m^2) by linear regression model from the PlanetScope primary image. A redline is provided as a reflectance line..... 39
Figure 3.5: Comparison of Linear and Non-linear (Exponential) models on PlanetScope subset data (a) and UAV data (b) with the use of bands, indices, and GLCM measures as predictor variables as computed from the initial model..... 41
Figure 3.6: Palatable grass biomass spatial maps as predicted by the linear model derived from the PlanetScope subset image..... 44
Figure 3.7: Palatable grass biomass spatial maps as predicted by the linear model derived from the UAV image..... 44
Figure 3.8: Scatterplot of the measured vs predicted palatable grass biomass (g/m^2) by linear regression model from the PlanetScope subset image (a) and by a UAV imagery (b) A redline is provided as a reflectance line..... 58

© University of Venda

List of Tables

Table 2.1: Spectral and Spatial resolution of the PlanetScope imagery…….. 11
Table 2.2: Classification results summary……...…….... 16
Table 3.1: Description and formula of selected variables, including raw bands, vegetation indices and texture features derived from PlanetScope imagery for mapping AGB……. 30
Table 3.2: Description and formula of selected variables, including raw bands, vegetation indices and texture features derived from UAV imagery for mapping AGB……. 31
Table 3.3: The initial results obtained from the PlanetScope big image for both the Linear model and Exponential model……..… 36
Table 3.4: The results obtained from the final linear regression model used for mapping AGB, with the validation metrics utilised to access model accuracy……. 37
Table 3.5: Obtained validation metrics values from the PlanetScope primary image……39
Table 3.6: Initial results obtained for both the PlanetScope subset and UAV data……... 40
Table 3.7: The results obtained from the final linear model used for mapping AGB derived from PlanetScope subset image, with the validation metrics utilised to access model accuracy……..... 42
Table 3.8: The results obtained from the final linear model used for mapping AGB derived from UAV image, with the validation metrics utilised to access model accuracy……... 43
Table 3.9: obtained validation metrics values from the PlanetScope subset image and UAV image…….. 46

© University of Venda

University of Venda
Creating Future Leaders

Table of Contents

Declaration i

Acknowledgments ii

General Abstract iii

List of figures iv

List of Tables v

CHAPTER 1: INTRODUCTION 1

1.1 Background to the Study 1

1.2 Rationale for the Study 3

1.3 Research Questions 3

1.4 Research outline 3

CHAPTER 2: 5

Fine-Scale Mapping of the Potential Communal Grazing Areas in the Vhembe East Villages, South Africa 5

2.1 Abstract 5

2.2 Introduction 6

2.3 Methods and Materials 9

2.3.1 Study Area 9

2.3.2 Field Data collection 10

2.3.3 Satellite data collection and pre-processing 11

2.3.4 Supervised Maximum Likelihood Classification 11

2.3.5 Classification Accuracy Assessment 12

2.3.6 Delimitation of the Study 13

2.4 Results 14

2.5 Discussion 17

2.6 Conclusion 20

CHAPTER 3: 22

© University of Venda

Testing the Performance of Linear and Non-linear Models for Mapping Palatable Grass Biomass Using the Unmanned Aerial Vehicle (UAV) and PlanetScope Data: A Case of Ka-Mavundani Village, Vhembe District 22

3.1 Abstract 22

3.2 Introduction 23

3.3 Methods and Materials 25
3.3.1 Study Area 25
3.3.2 Field Data Collection 26
3.3.3 Remote Sensing Techniques 27
3.3.3.1 PlanetScope data 27
3.3.3.2 UAV data 28
3.3.3.3 PlanetScope Subset data 28
3.3.4 Predictor Variable Selection and Extraction 28
3.3.5 Construction of palatable grass biomass evaluation models 32
3.3.6 Assessing Model Accuracy 34

3.4 Results 35

3.5 Discussion 46
3.5.1 Palatable grass biomass estimation using PlanetScope primary imagery 46
3.5.2 Palatable grass biomass estimation using PlanetScope subset imagery and the UAV imagery 48

3.6 Conclusion 50

CHAPTER 4: 52

Conclusion and Synthesis 52

4.1 Introduction 52

4.2 To map the potential communal grazing areas in the Vhembe East villages, South Africa 52

4.3 To test the performance of linear and non-linear models for mapping palatable grass biomass using the unmanned aerial vehicle (UAV) and PlanetScope Data 53

4.4 Limitations and Recommendations 53

REFERENCES 55

© University of Venda

CHAPTER 1: INTRODUCTION

1.1 Background to the Study

It is widely acknowledged that grass biomass is a direct indicator of rangeland quantity (Ramoelo *et al*., 2015) and grazing availability (Svinurai *et al*., 2021). Rangelands are defined as those types of land on which native vegetation is dominated by grasses, grass-like plants, forbs, and shrubs that are grazed or have the potential to be grazed. Rangelands contribute significantly to people's livelihoods and well-being throughout the world particularly in South Africa, through livestock production (Godde *et al*., 2020; Mbatha, 2021; Pfeiffer *et al*., 2022). Livestock production is a key element in rural livelihoods and decent quality rangelands support the sustainability of communal livestock. Rangelands also provide various natural resources in particular fuel wood, thatching grass, wild fruits, edible herbs, and medicinal plants, and these are harvested either for consumption or to sell (Vetter, 2013).

Grasses are some of the most important plant families on earth in terms of numbers of individuals, biomass, the area covered, diversity of habitats, and value to man. Over 30% of the land area of the earth is covered in natural grassland (Welti *et al*., 2020). South Africa's grassland the primary feed base for grazing livestock, which in turn provides the majority of low-income people with food, goods, and services that are essential for sustaining their livelihoods (Boval and Dixon, 2012). Livestock grazing, however, is built upon the palatability of grasses and will only happen when there is ample choice for food. Grass palatability is hence vital in livestock feedings, particularly cattle, for ensuring efficient animal production. Palatable grass biomass has long been perceived as an important characteristic of pastures, and for this reason, the evaluation of the biomass is thus crucial. It also aids in determining the availability of forage for animals and measures the effectiveness of management (Svinurai *et al*., 2021). Some of the common techniques that have been widely used in estimating, and monitoring, and managing vegetation include the field-based traditional methods and the remote sensing methods. The field-based traditional methods are often relied on due to their precision (Issa *et al*., 2020; Nguyen and Kappas, 2020). These in situ physical measurements are, however, constrained by various factors such as the inability to offer large spatial coverage (Rocchini *et al*., 2015), are time-consuming, laborious, and economically inefficient (Ali *et al*., 2015; Sibanda *et al*., 2021). Remotely sensed methods are currently complementing field measurements because of their ability to cover large spatial scales. The use of remote

© University of Venda

sensing technology has proven to be successful and effective in estimating vegetation biomass. It offers a time- and cost-efficient alternative to estimating and mapping biomass as an indicator of rangeland quality (Taddesse *et al*., 2020; Rhodes *et al*., 2022).

Evaluation of vegetation parameters using remote sensing (instruments that collect spectral reflectance measurements) has previously been conducted by satellites and aircrafts. However, due to technological advancements, lightweight multi- and hyper-spectral sensors carried by drones or unmanned aerial vehicles (UAV) have become widely available in recent years (Nasi *et al*., 2018). UAVs offer new alternatives to traditional remote sensing technologies. The newly advanced use of drone-based photogrammetric 3D data has been promising for biomass evaluation; furthermore, combining the 3D data and spectral data has greatly improved the results (Viljanen *et al*., 2018). Remote sensing data can be used to generate variables such as vegetation indices and biophysical variables which are suited for grassland investigations. While some studies have reported vegetation index to have shown to cause poor relationship with biomass, the use of spectral reflectance data, however, aids in the evaluation of biomass and has proven to be effective for palatable grass biomass estimation in terms of both total yield and productivity (Mutanga and Skidmore, 2004; Clementini *et al*., 2020; Naicker *et al*., 2024). Myriad studies have utilised Vegetation indices (VIs) adopted for multispectral or hyperspectral data (Nasi *et al*., 2018; Viljanen *et al*., 2018). A primary vegetation index (VI), such as the Normalised Difference Vegetation Index, is a commonly used index that has been used to evaluate grass biomass. They are widely used due to their ability to overcome the influences of atmospheric impurities and soil background and the viewing and zenith angle effects while magnifying the signature of vegetation (Sibanda *et al*., 2017). There is a correlation between vegetation indices such as the normalised difference vegetation index (NDVI), normalised difference water index (NDWI), and soil adjusted vegetation index (SAVI) and biomass and have been applied to palatable grass biomass.

Considering this background, the study aims to evaluate the biomass of palatable grass species in the communal rangeland using the integration of UAV data with high-resolution satellite data. The objectives of the study are as follows:

i. To map the potential communal grazing areas in the Vhembe East villages, South Africa.

© University of Venda

ii. To test the performance of linear and non-linear models for mapping palatable grass biomass using the Unmanned Aerial Vehicle (UAV) and PlanetScope data.

1.2 Rationale for the Study

Communal grazing areas, which are surrounded by poor communities, play a crucial role in supporting the livelihoods of many small-scale farmers in the Vhembe East villages. Despite their importance, poor documentation of the spatial distribution and biomass potential of these grazing areas do exist leading to challenges such as ineffective land management and overgrazing. Hence sustainable management of these areas is vital for rural livelihoods. Remote sensing technologies have been widely employed for biomass predictions, however, there is limited research on the application of high-resolution PlanetScope and UAV data for mapping communal grazing areas and the prediction of palatable grass biomass in communal rangelands. This study utilises the advancement in remote sensing technologies to narrow the gap by providing an integration of PlanetScope and UAV data offering unique opportunity to combine large-scale spatial coverage with fine-scale resolution. Mapping potential grazing areas is essential for sustainable land use and management, furthermore, knowledge on the distribution of palatable grass biomass is vital for ensuring efficient animal production.

1.3 Research Questions

The research questions of the study are as follows:

i. What is the extent and spatial distribution of potential communal grazing areas in the Vhembe East villages, as mapped with the use of high-resolution satellite imagery?
ii. Using remotely sensed data from PlanetScope and UAV, how well can linear and non-linear models predict biomass of palatable grass?
iii. Between the high-resolution PlanetScope imagery and the fine-scale UAV data, which dataset is better suited for palatable biomass mapping in Vhembe East villages?

1.4 Research outline

This thesis consists of four (4) chapters, as shown in Figure 1.1: Chapter 1 presents the general background of the study, aim, and objectives. Chapter 2 presents the mapping of potential communal grazing areas in the Vhembe East villages. Chapter 3 tested the performance of linear and non-linear models for mapping palatable grass biomass using the Unmanned Aerial Vehicle (UAV) and PlanetScope data. Chapter 4 presents the synthesis of the study. Each chapter has its own introduction, methods, results, discussion, conclusions, and reference list.

© University of Venda

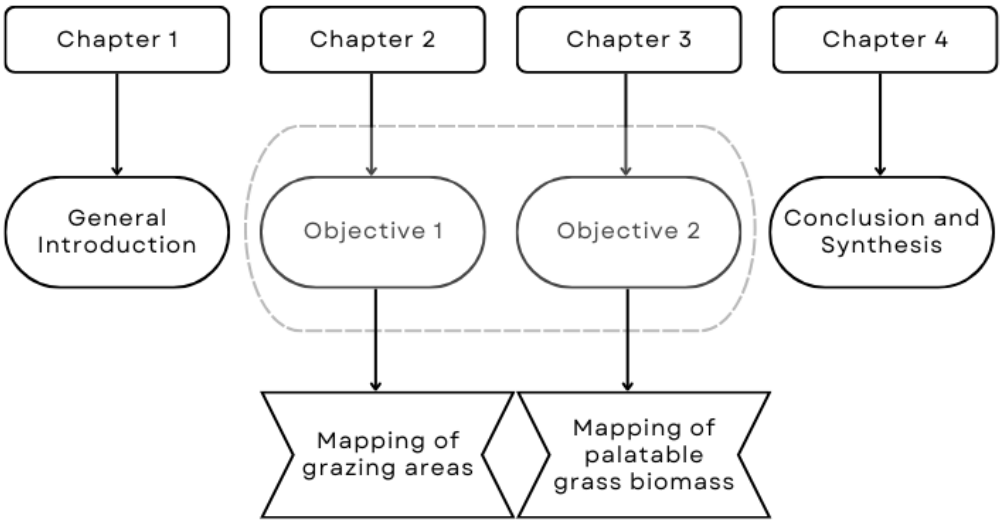


Figure 1.1 Flowchart of the thesis outline used in the study.

© University of Venda

CHAPTER 2:

Fine-Scale Mapping of the Potential Communal Grazing Areas in the Vhembe East Villages, South Africa

2.1 Abstract

Communal rangelands are an important ecosystems for sustaining livelihoods both on a global scale and within South Africa. However, they face significant threats primarily from overgrazing and mismanaged fire regimes. This study thus investigated the potential of PlanetScope data for mapping the potential communal grazing areas within communal areas at fine-scale resolution using the Supervised maximum likelihood classification algorithm. The model showed a high overall accuracy of 99.29% and Kappa of 0.98 with user's and producer's accuracies ranging from 93.31% to 100%. Findings revealed that the study area was dominated by grazing areas covering 50% of the area which is about 33 695 hectares (ha), followed by built-up areas (26%) and woodlands (12.70%). Detailed classification and grazing area maps were produced thus revealing important insights into the distribution of communal grazing areas within the study site. The ML classification model displayed an effective capability in accurately delineating between various land cover types ensuring for precise mapping of communal grazing areas. The classification accuracy assessment produced from the study indicates the reliance of the model in the mapping approach. This study offers a robust and data-driven approach to defining grazing areas while providing valuable knowledge for stakeholders involved in communal land management.

Keywords: Communal grazing areas, fine-scale mapping, PlanetScope data, Supervised Maximum Likelihood (ML) classification,.

© University of Venda

2.2 Introduction

Communal rangelands are ecosystems that are communally owned and managed, as opposed to private individual land ownership, and are areas where agriculture is largely subsistence-based. These rangelands lack clear guidelines for managing grazing areas and they are commonly used and shared by the community without any management (Letsoalo, 2019). Communal rangelands are an essential resource for millions of people worldwide, particularly in developing countries. According to the World Bank (2018) approximately 3.45 billion people live in rural areas, and 90% of them are small-scale farmers whose primary source of income comes from agriculture (Sikhweni and Hassan, 2014a). These rangelands are surrounded by poor communities (Singh *et al*., 2018) and they play a crucial role in supporting the livelihoods of many small-scale farmers, who rely on them for food, income, cultural identity, and livestock production (Steinfeld *et al*., 2006). About 40% of global agriculture's gross domestic product is generated by the livestock sector (Tavirimirwa *et al*., 2019). A study by (Tavirimirwa *et al*., 2019) reported that small-scale farmers in Southern Africa rely heavily on communal rangelands to produce livestock. This is notably true in South Africa, where communal farming remains an important part of the country's agricultural sector and plays a crucial role in providing food security and income to rural communities.

According to a study conducted by the Department of Agriculture, Forestry and Fisheries (DAFF) in South Africa, approximately 33% of the national cattle herd is found in the small-scale sector (DAFF, 2013). Additionally, an estimated 80% of agricultural land in South Africa is suitable for extensive grazing. Despite their significance, communal rangelands, however, face various problems that hinder their sustainable use and management. For example, a study by (Sinthumule and Mzamani, 2019) reported that a number substantial number of households in Josefa and Matiyani villages in Limpopo, South Africa, largely depend on subsistence small-scale farming, of which keeping cattle serves as their primary farming activity. One of the major problems of communal rangeland is overgrazing (Bolo *et al*., 2019) which in communal lands is a significant issue that can have severe consequences for communities that depend on them. Overgrazing by cattle promotes the spread of undesirable plant species and bush encroachment as desirable palatable grass species are eliminated, all of which are signs of rangeland degradation (Mekuria, 2013; Fenetahun *et al*., 2021). This may lead to reduced livestock productivity, contribute to social conflicts within communities, and have further consequences for local communities that rely on livestock for their livelihoods. Hence,

© University of Venda

sustainable grazing practices are crucial in maintaining communal rangeland quality and ensuring the livelihoods of rural communities, as livestock production is dependent on rangeland quality.

Communal rangelands encompass vast areas of land used for communal grazing (Sandhage-Hofmann *et al*., 2015); hence, it is crucial to effectively manage these areas to maintain their productivity and sustainability (Masiteng *et al*., 2003; Bennet and Barrett, 2007). In recent years, informed decision-making, and sustainable management techniques have improved with the rising understanding of the importance of accurate information on the spatial distribution and condition of communal grazing areas (Kellner and Moussa, 2019; Kakembo and Ndou, 2019). Knowledge of the distribution of palatable grass species in communal grazing areas is essential for livestock management (Hampson *et al*., 2022) as it helps to understand the ecology of the area and how to manage livestock more effectively (Waudby *et al*., 2013). The evaluation of grazing potential in communal grazing areas is a crucial aspect of sustainable land management. Certain areas of rangelands are characterised by low potential grazing, while others are characterized by high potential grazing; therefore, to avoid overgrazing and the deterioration of rangelands, it is important to estimate the grazing potential of the area (Bailey, 2004). The livelihoods of many communities in South Africa depend on the efficient management and sustainable use of these resources, which can only be achieved through mapping and monitoring community grazing land. Moreover, mapping and monitoring potential communal grazing areas is essential for sustainable land use, land tenure and ownership, resource management, and conservation in South Africa (Awuah *et al*., 2020; Gusha *et al*., 2023).

Traditional methods of mapping communal grazing areas have posed significant challenges as they rely on ground-based surveys. These surveys involve in-situ assessments and manual data collection, which require substantial time, effort, and resources (Singh *et al*., 2018), making them difficult to implement in larger and remote areas. However, in recent years, advancements in remote sensing techniques, such as satellite imagery, have offered promising opportunities to overcome these challenges. According to their unique spectral characteristics, vegetation with unique spectral features can easily be identified from remotely sensed images, and for this reason, satellite remote sensing is ideally suited for communal grazing areas (Sibanda *et al*., 2021). A study by Svoray *et al*., (2013) also revealed the ability of remote sensing to offer significant opportunities for observing, monitoring, estimating, and also understanding

© University of Venda

the potential ecological threats within rangelands. According to (Hunt *et al*., 2003) rangeland managers would prioritise a remote sensing technique that classifies an area based on the succession status of the grass species present rather than relying solely on generalised land-cover classification. Nevertheless, the precise distributions of specific plant species remain a persistent challenge challenging to ascertain (Hilbert, 2001).

Land use and land cover classification is an important aspects of land resource management. With the aim of categorising and mapping distinct types of land cover (such as vegetation, water, and bare soil) that occur in a particular area. This image classification technique is usually performed using remote sensing data, such as satellite images. Efficient identification and examination of land use and land cover have recently been made possible with the advancements of these remote sensing and geographic information systems as compared to the past (Kamwi *et al*., 2017). Different classification techniques exist that can be used to accurately classify different land use and land cover classes, these include supervised and unsupervised classification. The maximum likelihood (ML) is a popular supervised machine learning algorithm in remote sensing and image classification (Patil and Kambekar, 2022) that has probability theory as its foundation (Malahlela *et al*., 2014). It assesses the probability that each pixel, based on the spectral characteristics, belongs to a specific class and then places that pixel in the class with the highest probability (Traore *et al*., 2018; Koko *et al*., 2021; Patil and Kambekar, 2022). According Kaul and Ingle (2012) several studies have reported maximum classification accuracies of land use land cover classification to have been acquired through the use of, several studies have reported maximum classification accuracies of land use land cover classification to have been acquired through the use of ML classification. This classifier has previously been used in mapping communal grazing areas. For instance, a study by Awuah *et al*. (2020) successfully used an ML classifier to map grazing lawns in southern African savannahs and obtained accurate results with the utilisation of WorldView-3 imagery. Another study by Tsegaye *et al*. (2010) employed ML classification with the use of Landsat imagery in mapping and analysing changes in land use and land cover while defining grazing areas in the Afar rangelands of Ethiopia. Some studies, such as Tsegaye *et al*., (2010) have utilised the ML classifier and, however, concentrated on regional or national scale mapping. Mapping grazing areas at finer spatial scales is crucial to enable local villagers or communities to overcome their challenges regarding land management practices. Thus, the aim of the study is fine-scale mapping of the potential communal grazing areas in the Vhembe east villages, South

© University of Venda

Africa. The objective of the study is, therefore, to map potential communal grazing areas within the Vhembe East villages.

2.3 Methods and Materials

2.3.1 Study Area

The study area is situated in the Collins Chabane Local Municipality (CCLM). This local municipality lies within the Vhembe District Municipality in the far north of the Limpopo Province of South Africa (**Figure 2.1**). The Municipality is one of the four local municipalities in the district and makes up 20% of its geographical area with a jurisdiction area covering 5 467.22 km² (22° 35′ S 30° 40′ E). The study area includes the following villages: Bevhula, Botsoleni, Dinga, Gijamandzini, Gijana, Govhu, Green farm, Jerome, Jilongo, Joseph, Ka-Matiani, Ka-Mavundani, Ka-Nghezimani, Ka-Sunduza, Lombard, Mabaligwe, Mabayeni, Malamulele, Malamhala, Makumeke, Maphophe, Masobye, Merve, Mchipisi, Mhinga, Mtititi, Nkavele, Ntlhaveni, Nghomunghomu, Peninghotsa, Readhouse, Saselamani, Shigalo, Xaswita, Xitlhelani. The unemployment rate in this area is 45% (Murei *et al*., 2022) which leads to communities within the area being highly dependent on their communal land for cattle grazing, which contributes to their livelihoods (Sikhweni and Hassa, 2014a). Subsistence farming, raising animals, and human settlement are the principal land uses in the region (Chaminuka *et al*., 2014; Sikhweni and Hassan, 2014a). The site is characterised by the conversion of croplands to grazing areas and the open lands and farms are used by livestock farmers as grazing lands.

© University of Venda

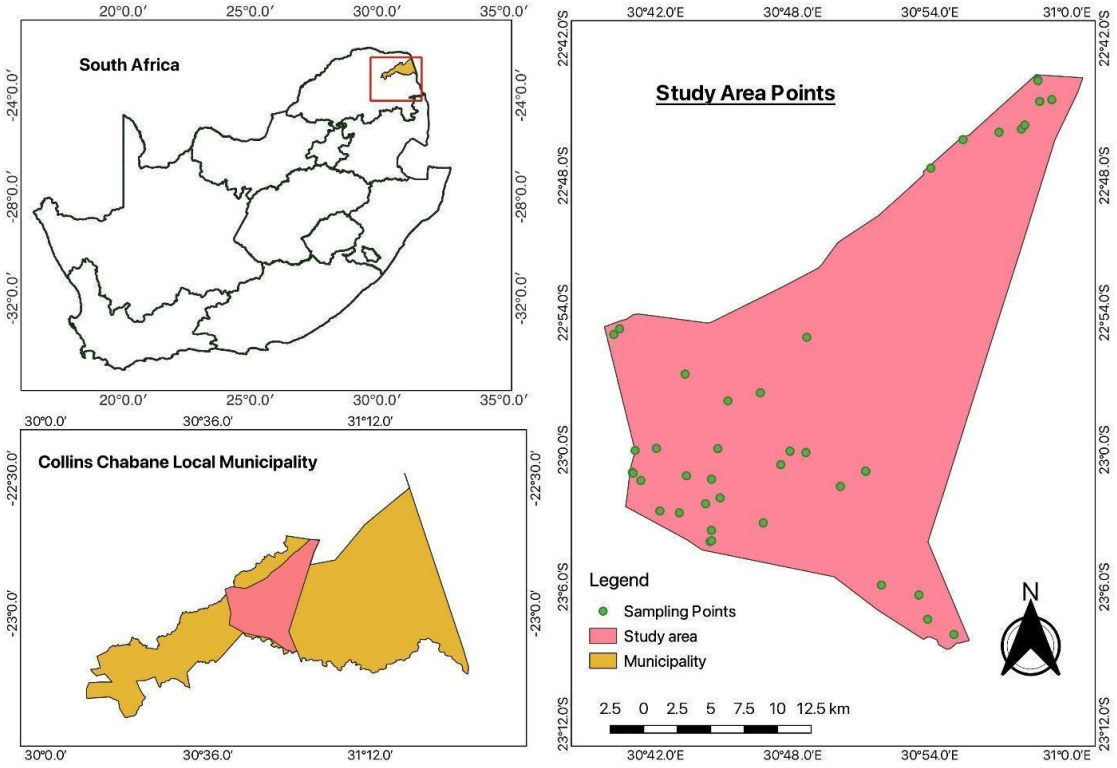


Figure 2.1: The location of the study area with sampling areas.

2.3.2 Field Data collection

The field measurements were conducted between September and October 2022 which aligns with the end of dry season and beginning of early wet season in Vhembe District. This is the period when there is spares vegetation, visible grazing and minimal rainfall. During the fieldwork, a total of 36 sampling areas measuring 30m × 30m were randomly established. Within each of these areas, two plots were randomly selected by placing a 5m × 5m square wire frame on the field. Thus, resulting in a total of 72 sub-plots measuring 0.5 × 0.5m. Grass species were then identified and recorded within the 5m × 5m sub-plots. A total of n = 172 grass samples were randomly collected within the study area and divided into 70% (n = 120) and 30% (n = 52) for training and validation, respectively. The vegetation coverage was visually estimated within the 30 m and 0.5 m points. The spatial distribution of the sampling points is shown in **Figure 2.1**. A handheld standard Garmin eTrex 20™ Global Positioning System (GPS) was employed to record the coordinates of the points with a maximum accuracy of 3 m. It is worth noting that although field data was collected in the study, full utilisation and analysis of the data will

© University of Venda

be covered in the following chapter, hence making it an important part of the upcoming analysis.

2.3.3 Satellite data collection and pre-processing

PlanetScope imageries were selected as the data source for this study because of their high spatial resolution and short revisit time (Vrieling *et al*., 2022). The Planet Labs-operated PlanetScope satellites are a constellation satellite consisting of 180+ CubeSats which are in a sun-synchronous orbit with an equator crossing time between 9:30 and 11:30 (local solar time) (Planet Labs Inc, 2023). The PlanetScope sensors acquire spectral imagery in four spectral bands (**Table 2.1**): blue (455–515 nm), green (500–590 nm), red (590–670 nm), and near infrared (NIR) (780–860 nm) (Cheng *et al*., 2020). These satellites are commercial CubeSats, which are quickly emerging as essential tools for mapping the Earth's surface (Frazier and Hemingway, 2021). Previous studies have successfully utilised PlanetScope (PS) data in mapping and monitoring grazing areas and rangelands (Lui *et al*., 2019; Dos Reis *et al*., 2020) as well as land-cover classification (Parente *et al*., 2019; Andreatta *et al*., 2022; Lefulebe *et al*.,2022). The imagery with a 3 m spatial resolution is a CubeSat multispectral cloud-free image, which is a surface reflectance product that has been atmospherically corrected by Planet Labs covering the study area. It was acquired on the 1st of October 2022 from Planet Labs. Images obtained were merged into a mosaic for subsequent analytical purposes in Quantum GIS (version 3.28.3) software (QGIS Development Team, 2022).

Table 2.1: Spectral and Spatial resolution of the PlanetScope imagery

PlanetScope Band	Spectrum Region	Wavelength (nm)	Spatial Resolution
Band_1	Blue	455-515	
Band_2	Green	500-590	3m
Band_3	Red	590-670	
Band_4	NIR	780-860	

2.3.4 Supervised Maximum Likelihood Classification

The study explored the application of maximum likelihood classification (MLC), a supervised classification algorithm, to map grazing areas. The supervised classification

© University of Venda

was conducted using the SCP Dock tool of the Semi-Automatic Classification Plugin (SCP) within the QGIS software. Maximum likelihood is a robust machine learning algorithm in remote sensing and image classification (Patil and Kambekar, 2022) that has probability theory as its foundation. It assesses the probability that each pixel, based on the spectral characteristics, belongs to a specific class, and then places that pixel to the class with the highest probability (Traore *et al*., 2018; Koko *et al*., 2021; Patil and Kambekar, 2022). With each land cover class, the regions of interest (sample training data) were selected as identified in the satellite image and were manually labelled with their corresponding land cover class. This supervised classification relies on pre-processing and post-processing techniques to accurately produce a land use map. The study used a high-resolution PS data as input data for the classification process to develop a land use land cover map of the study area, which is the main product of remote sensing image classification, as shown in **Figure 2.2**. Five land use land cover classes were identified over the study area and utilized as the training data: a) Water bodies, b) Vegetation, c) Built-up, d) Grazing areas and e) Woodlands. The Supervised maximum likelihood classification was applied to the input data using the selected training data as its reference. The selection of training data improves the accuracy of the classification results (Chen *et al*., 2020; Zhang *et al*., 2023).

2.3.5 Classification Accuracy Assessment

Accuracy assessment is a crucial element in image classification that determines the quality and reliability of a land cover classification's performance (Bharatkar and Patel, 2013; Schill *et al*., 2021). The accuracy of ML classification can be quantified by employing the area-based error matrix method, which is what has been implemented in the study. Area-based error matrix is an approach that measures the classification accuracy by calculating various metrics such as overall accuracy, User's accuracy, Producer's accuracy and Kappa coefficient (Gallant *et al*., 2021). It compares the classified land cover classes produced by the maximum likelihood algorithm with the reference data that reflect the true land cover classes. Overall accuracy is a ratio of overall correctly classified pixels against the total number of pixels in an image. This is how accurately the MLC algorithm has assigned the pixels to their correct land cover classes. The expression of the Overall accuracy is represented by the equation (1):

$$Overall\ accuracy\ (\%) = \frac{Sum\ of\ correctly\ classified\ pixels}{Total\ number\ of\ reference\ pixels} \quad (1)$$

The Users accuracy is the ratio of the pixels correctly classified for a given class relative to the total number of pixels classified as that class, while Producer's accuracy is the ratio of the correctly classified pixels for a specific class relative to the total number of pixels that truly belongs to that class. User's accuracy and Producer's accuracy are obtained from the equations (2) and (3) respectively:

© University of Venda

$$User's\ accuracy\ (\%) = \frac{Number\ of\ correctly\ classified\ pixels\ in\ each\ class}{Total\ number\ of\ pixels\ classified\ in\ that\ class} \quad (2)$$

$$Producer's\ accuracy\ (\%) = \frac{Number\ of\ correctly\ classified\ pixels\ in\ each\ class}{Number\ of\ reference\ known\ to\ that\ class} \quad (3)$$

The Kappa coefficient, on the other hand, measures the agreement between the classified image and the reference data, considering the possibility of the expected results if the classification were random. The Kappa values range from 0 to 1, where 1 denotes complete agreement and 0 denoting no agreement beyond randomness. The Kappa coefficient is given off by the equation (4) as stated by (Bharatkar and Patel, 2013).

$$K = \frac{P_0 - P_c}{1 - P_c} \quad (4)$$

Where: P_0 = proportion of units which agree (observed accuracy), = overall accuracy, and P_c = proportion of units for expected chance agreement (chance agreement).

2.3.6 Delimitation of the Study

The study focused on mapping potential communal grazing areas within the Vhembe east villages. the study site covers about 35 villages namely: Bevhula, Botsoleni, Dinga, Gijamandzini, Gijana, Govhu, Green farm, Jerome, Jilongo, Joseph, Ka-Matiani, Ka-Mavundani, Ka-Nghezimani, Ka-Sunduza, Lombard, Mabaligwe, Mabayeni, Malamulele, Malamhala, Makumeke, Maphophe, Masobye, Merve, Mchipisi, Mhinga, Mtititi, Nkavele, Ntlhaveni, Nghomunghomu, Peninghotsa, Readhouse, Saselamani, Shigalo, Xaswita, Xitlhelani. It encompasses an area of 66981.89 hectares (ha) in total. Communal rangelands were of interest as they are a source of income to many around the area as they provide areas suitable for livestock grazing. Therefore , only grass species were considered and all other vegetations were excluded from the analysis. The study employed a combination of field measurements (conducted from September to October 2022) and remote sensing technology such as satellite data from the PlanetScope imagery (acquired on the 1st of October 2022). The study employed the maximum likelihood (ML), a popular Supervised image classification algorithm, to classify different land use types within the study; and to generate communal grazing areas map.

© University of Venda

2.4 Results

The land cover classification was conducted with the use of a PS data with resolution of 3 m. In accomplishing this, a ML classification was employed and was found to be reliable in mapping grazing areas. **Figure 2.2** shows a comprehensive depiction of the classification map produced from the ML classification method used in the study. The classification map visually depicts the spatial distribution of land cover classes within the study area with each colour on the map corresponding to the specific land cover class. The map clearly provides an overview of the land cover classes' extent. The classification model was assessed with the use of an area-based error matrix which yielded high accuracy results. **Table 2.2** presents the results for overall accuracy, user's accuracy, producer's accuracy, and Kappa coefficient, i.e. Kappa hat. The overall accuracy of the classification was 99.29% with high user's and producer's accuracies ranging from 93.31% to 100% for the different land cover classes. The land cover classification results showed the dominance of the land cover classes as depicted by their various area sizes in **Table 2.2**. Grazing areas were dominant land cover classes, covering 50% of the study area, followed by built-up areas (26%) and waterbodies with the least (0.21%). The accuracy assessment was further evaluated using the Kappa coefficient which was obtained at 1 (Kappa hat classification of 0.98). Based on the land cover classification results, the grazing area map (**Figure 2.3**) illustrates the specific locations that have been classified as grazing areas as represented by the value of 1 and non-grazing sites represented by the value of 0. The results obtained in this model are indicative of the potential of PlanetScope imagery for mapping grazing areas and provide comprehensive insights into the distribution of the different land use spatial patterns. The land classes' area sizes (in percentage) are depicted by **figure 2.4** with grazing areas having the most area size and water bodies having the least area size.

© University of Venda

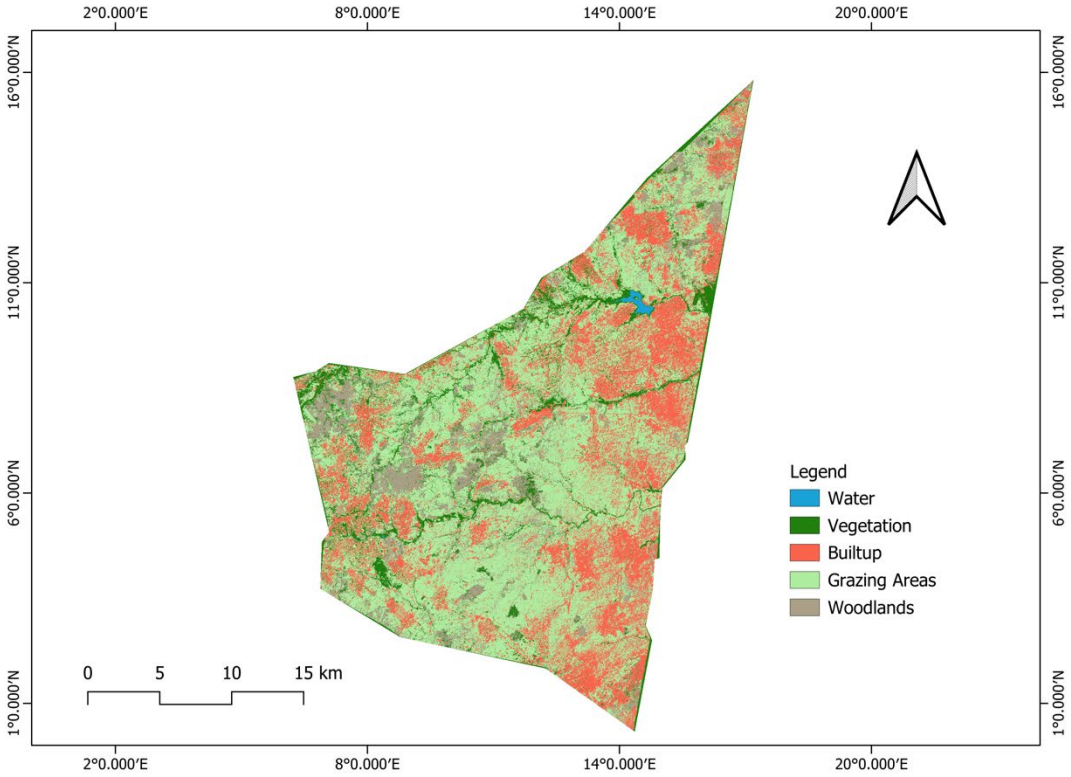


Figure 2.2: Classification map of Vhembe east villages from PlanetScope imagery using Maximum likelihood Classifier with five class categories: Water, Vegetation, Built-up areas, Grazing areas, and Woodlands.

© University of Venda

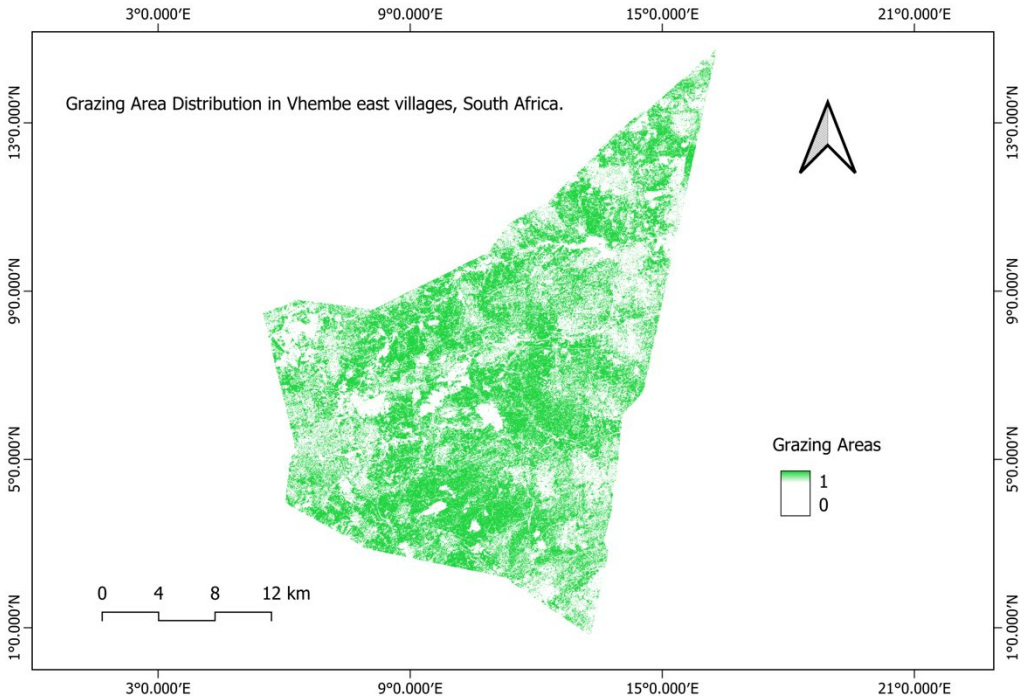


Figure 2.3: Grazing areas distribution within the study area.

Table 2.2: Classification Results summary

Land Cover Class	**Area size (%)**	**Area size in hectors**	**User's Accuracy (%)**	**Producer's Accuracy (%)**
1. Water	0.21	141.63	100	100
2. Vegetation	9.85	6595.91	100	93.31
3. Built-up	26.94	18041.89	100	100
4. Grazing areas	50.30	33695.05	100	100
5. Woodlands	12.70	8507.41	94.44	93.69
Overall accuracy (%)		99.29		
Kappa hat classification		0.99		

© University of Venda

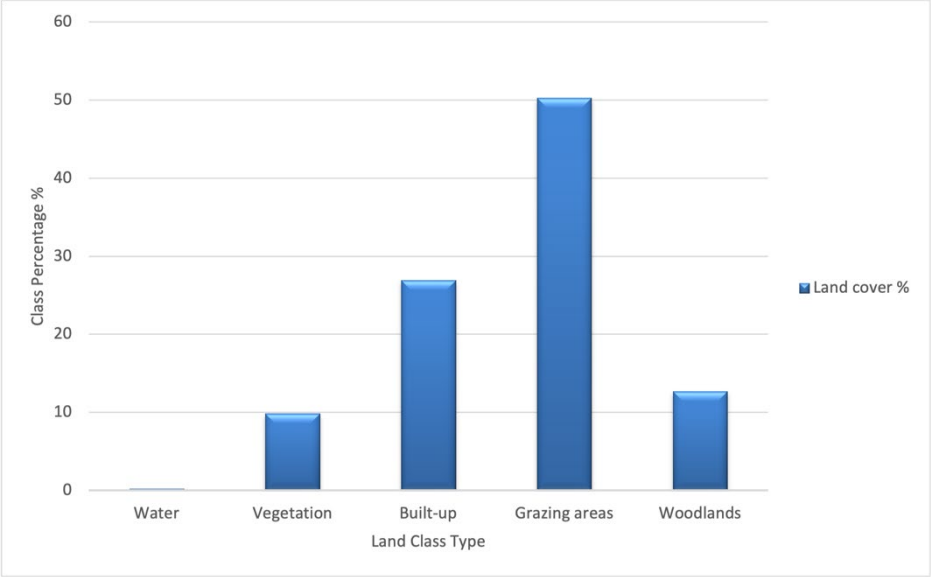


Figure 2.4: Chart depicting land cover classes as per the area size they hold within the study area.

2.5 Discussion

This study aimed to map the communal grazing areas within the Vhembe East villages using high-resolution PlanetScope data. The study's findings are essential for identifying possible grazing areas in the community rangelands. Mapping of grazing areas allows for a comprehensive understanding of the extent and locations of these areas. To achieve accurate mapping of grazing areas, the study employed the use of ML classification which is a supervised classification technique. The classification process produced a precise classified land cover map (**Figure 2.2**) with five land cover classes namely: Water, Vegetation, Built-up areas, Grazing areas, and Woodlands. The land cover classes within the study area have successfully been delineated as represented by the unique colours on the map. As a result, the study offers useful spatial data on potential grazing areas and information that not only smallholder farmers but also individuals in the community could utilize to make well-informed planning decisions. An accuracy assessment was performed to validate the classification model. The high user's accuracies and producer's accuracies obtained (**Table 2.2**) ranging from 93.31% to 100% is indicative of an exceptional performance of the model in identifying the different land cover classes within the study and more importantly, the grazing areas with 100% for both the user's accuracy and producer's accuracies. This is a precise reflection of the model's effectiveness in delineating the grazing areas from other land cover types in the study.

© University of Venda

The model yielded a high overall accuracy of 99.29%, revealing a robust correlation between the classified land cover types and the actual data. The Kappa hat obtained at 0.99 further strengthens the reliability and precision of the classification model as it suggests that the model effectively identifies the different land cover types and the grazing areas within the study area. Furthermore, the classification has revealed the dominance of each land cover class within the study area, with grazing areas as the predominant land type accounting for 50.30%, followed by built-up areas at 26.94%, woodlands covering 12.70%, vegetation at 9.85%, and lastly, water bodies accounting for 0.21% of the study area. The grazing areas cover 33695.05 of 66981.89 hectares (ha) that make up the study's total area. The classification map produced is evident that the grazing areas are dispersed evenly across the study area.

The findings from the study are significant and in line with previous studies that have examined the use of ML and highlighting its robustness in land use classification. In their study (Koko *et al*., 2021) employed ML classification in classifying land use changes in Nigeria. Their analysis revealed significant land use changes and urban expansion in the study area. A study by Norovsuren *et al*. (2019) applied ML in classifying land cover within the Khandgait Valley in Mongolia in 2000 and 2019. They obtained high overall accuracy of the land cover classification of 86.5% and 89.0% for 2000 and 2019, respectively. Another study by Awuah *et al*. (2020) conducted similar studies and achieved a high accuracy of 91.1% in classifying grazing lawns in Southern African savannahs. A study by (Palamuleni *et al*., 2007) compared the ML and fuzzy classifiers and found that the use of the ML classifier in mapping grazing areas outperformed the fuzzy classifiers with a higher overall accuracy of 87%, resulting in accurate land cover classification. Other studies exhibit notable similarities in terms of outstanding overall accuracy retrieval. (Nawaz *et al*., 2015) retrieved 99.17% accuracy with ML outperforming other classifiers; (Abbas and Jaber, 2020) used the ML classification and Support Vector Machine in extracting land cover maps and obtained an overall accuracy of 91.5%; and (Sisodia *et al*., 2014) obtaining an overall accuracy of 93.75%. These studies demonstrate the effectiveness of the ML classification in mapping grazing areas. Additionally, PS data has been used by several studies in rangeland management. A study by (Liu *et al*., 2019) used PS data in combination with a small unmanned aerial system to map forage production in grazing areas. According to a study by (Acharki, 2022) results show superior performance from the PS data in classifying land cover as compared to Landsat-8 and Sentinel-2 while achieving an overall accuracy of over 97%.

© University of Venda

Although the study has demonstrated the use of PlanetScope data in mapping grazing areas, opportunities do exist to improve the PlanetScope classification model for attaining robust fine-scale resolution to estimate the potential grazing areas. The emergence of fine-scale resolution data, as proof of the advancements of remote sensing technology, has allowed for the collection of more detailed land information, and this has offered researchers with high detailed and accurate spatial information that provides detailed information about land as compared to coarse resolution data resulting in a decline in the use of coarse resolution data. Nonetheless, there is still a need for coarse resolution data as they are often affordable, easier to process and provide data over large areas that fine-scale resolution may not be able to project. While PlanetScope data offers fine-scale resolution satellite images that enable detailed spatial analysis, as with land cover classification, they require consideration of other factors that may impact the quality and accuracy of the data.

Several socio-economic factors that can be drawn from the study do exist. The study highlighted the importance of communal grazing areas for smallholder farmers and individuals in the Vhembe East villages, who rely on them for their livestock production. Therefore, there is a need for recognition of the importance of communal grazing areas in the study and a need to adopt an approach (such as the implementation of sustainable grazing management programs) that will promote sustainable grazing lands and livestock management. The findings on potential grazing areas can assist these individuals in making well-informed decisions, consequently improving their livestock productivity. The study employed the use of remote sensing technology in mapping of potential communal grazing areas, which has positive effects. The application of remote sensing technology offers cost-effective, reliable, and accurate data. Nonetheless, such technology requires specialised skills and expertise, which may not be easily accessible to smallholder farmers in the Vhembe east villages. The areas that were considered to have grazing value were observed during the field investigation to be overgrazed/highly grazed, and either had grazing indicators such as cow dung/eaten shoots and cattle grazing on site. The adoption of sustainable grazing strategies by smallholder farmers in the villages of Vhembe is hence vital to combat such challenges, moreover, an ecological balance can be maintained by effective management of the livestock grazing pressures.

While the findings of the study are essential, there are a number of limitations and potential challenges to consider. Firstly, due to ML classification's sensitivity to the selection of training classes, careful selection of the samples ought to be done to avoid

© University of Venda

biased results, which may have a significant effect on the accuracy of mapping grazing areas (Sisodia *et al*., 2014; Acharki, 2022). Secondly, the study was centred on the ML classification without exploring its comparison to other classification algorithms, which would either give a similar or different perspective unfamiliar perspective of the strength of the ML classifier. Thirdly, it is worth noting that the study initially presented limitations that resulted in the transition from the use of a logistic regression model in mapping potential grazing areas to a classification based strategy. The logistic regression model failed to produce a meaningful output map, and after several attempts, it became certain that the use of logistic regression and PlanetScope data in mapping the grazing areas within the study had limitations that hindered the accurate mapping of grazing areas. The ML algorithm, on the other hand, has potential enormous potential for extracting land cover data, and the transition was driven by its capability and accuracy in handling complex data (Palamuleni *et al*., 2007; Abdullahi *et al*., 2020). Future studies that address these issues will offer a better understanding of the potential grazing areas and their impact, not forgetting the capabilities offered by the imagery. Results from the study denoted the potential of PlanetScope data in mapping communal rangelands reliably. The communal grazing areas in the Vhembe east villages have been long used for livestock grazing. However, to the best of our knowledge, their distribution has not been recorded, which may be a result of findings from a study by (Sebola *et al*., 2020), who reported ineffective governance and management of communal lands in Vhembe villages. this lack of documentation becomes a key gap in sustainably managing the communal grazing areas.

2.6 Conclusion

The aim of the study was to map communal grazing areas within the study area with the use of PS data and advanced classification techniques. The following observations obtained in this study served as the foundation for the conclusion:

- The model obtained an overall accuracy of 99.29% and Kappa coefficient of 0.98, with user's and producer's accuracies ranging from 93.31% to 100%, highlighting reliability of classification model for mapping potential communal grazing areas.
- The dominate land cover class was shown to be grazing areas which accounting for 50% (33 695 hectares) of the area, followed by built-up areas 26.94%, woodlands covering 12.70%, vegetation at 9.85% , and water bodies with the least 0.21% of the study area.

© University of Venda

- The output detailed classification and grazing area maps produced offers valuable insights into spatial distribution of the grazing areas.
- This research study offers knowledge in mapping communal grazing areas thus promoting future research in the study area that could improve the feed for livestock, well-being of the communities and the country's economy at large.

The current chapter successfully mapped the communal grazing areas. However, it remains to be assessed what the distribution of the grass biomass is in the mapped communal grazing areas. For this reason, the following chapter aims to look into testing the performance of linear and non-linear models for mapping above ground biomass with the use of unmanned aerial vehicle (UAV) and PlanetScope data.

© University of Venda

CHAPTER 3:

Testing the Performance of Linear and Non-linear Models for Mapping Palatable Grass Biomass Using the Unmanned Aerial Vehicle (UAV) and PlanetScope Data: A Case of Ka-Mavundani Village, Vhembe District

3.1 Abstract

Accurate mapping of palatable grass biomass is an important phenomenon as it provides a crucial understanding of the health of rangelands while facilitating effective land management and sustainable resource utilisation of the health of rangelands while facilitating effective land management and sustainable resource utilisation. This study tested the performance of the linear and non-linear regression models in mapping of palatable grass biomass using remotely sensed data derived from the UAV and PlanetScope imagery. Several models were developed and tested with the use of spectral bands, vegetation indices and grey-level co-occurrence matrix (GLCM) features derived from both sensors. This was conducted to obtain the most accurate models for predicting and mapping palatable grass biomass within the study area. The findings showed that the linear regression models consistently and slightly outperformed their non-linear regression models counterparts. The results from the PlanetScope primary data yielded a root mean squared error (RMSE), mean absolute error (MAE) and coefficient of determination of 2.16, 1.69 and 0.11, respectively. These findings suggest the potential for prediction improvement of the model. The study reveals that the linear regression models from the PlanetScope subset image, as compared to the linear regression models from the UAV imagery, had superior performance and had acquired RMSE of 2.36, MAE of 3.22 and R^2 of 0.35 for the subset image, and an RMSE, MAE and R^2 of 9.83, 6.56 and 0.23, respectively for the UAV image. This means that the relationship between remote sensing variables and the distribution of palatable grass biomass could be explained by the linear regression model from the subset data as compared to the UAV data. The remote sensing variables derived from the subset data offer a better estimation of the palatable grass biomass. The study demonstrated the potential of using advanced remote sensing techniques and regression models to estimate palatable grass biomass.

Keywords: linear regression, non-linear regression, palatable grass biomass, PlanetScope, remote sensing, UAV

© University of Venda

3.2 Introduction

Rangelands constitute a vast and diverse portion of the Earth's surface, offering significant spatial variation in soil type, vegetation composition, and structure (McGranahan and Kirkman, 2013). Communal rangelands, characterised by native vegetation and dominated by grasses, grass-like plants, phorbs, and shrubs, not only play a significant role in maintaining biodiversity and ecosystem services but also play a crucial role in supporting the livelihoods of surrounding rural communities (Mdiya *et al*., 2021). They are managed as natural ecosystems to produce grazing livestock and wildlife (Mangani *et al*., 2022) and sustains livestock by providing abundant forage of superior quality (Getabalew and Alemneh, 2019; Letsoalo, 2019). Within these environments, biomass is a key determinant of the quantity and variety of living organisms, including vast differences in amounts of dead and green biomass. Biomass, in this context, refers to the palatable grass biomass available for grazing cattle. The biomass of palatable grass has long been perceived as an important characteristic of pastures, and for this reason, the evaluation of the palatable grass biomass is thus crucial as it represents the main food source for livestock grazing. It also aids in determining the availability of forage for animals and measures the effectiveness of rangeland management (Svinurai *et al*., 2021).

Palatable grass biomass is a key indicator, especially in communal rangelands, for the productivity and health of rangelands. The mapping of palatable grass biomass in communal rangelands is an important aspect of managing and understanding these landscapes. The potential to accurately assess and map palatable grass biomass in such communities is crucial for effective land management and sustainable resource utilisation, preventing overgrazing and ultimately ensuring an adequate forage base for livestock (Mudau *et al*., 2022). Due to its major impact on the livelihoods of rural communities who rely on the rangelands for their subsistence, palatable grass biomass management of these rangelands is of vital importance (Gorade and Datar, 2014; Rapiya *et al*., 2023). While communal rangelands provide vital grazing resources, the productivity and quality of palatable grass biomass are altered by recurrent droughts and changing climatic conditions (Mudau *et al*., 2022). Thus, inconsistent and outdated information, lack of large-scale quantification, and mapping efforts in rangelands bring about uninformed decision-making regarding the shared rural communal lands, furthermore restricting efficient monitoring of grazing capacity (Jamsranjav *et al*., 2019; Fenetahun *et al*., 2021). Moreover, in many cases, the mapping of palatable grass biomass in such areas presents unique challenges. Challenges include the variability in vegetation, limited accessibility, and resource constraints. Therefore, precise and efficient assessment techniques for mapping are required. Most assessments relied on infrequent field surveys or outdated vegetation maps (Taddese *et al*., 2020), offering limited spatial information about current forage availability and conditions to facilitate adaptive planning. The field-

© University of Venda

based traditional methods are often relied on due to their precision (Issa *et al*., 2020; Nguyen and Kappas, 2020) and remain the primary way of mapping palatable grass biomass, but they are, however, time-consuming and labor-intensive (Sibanda *et al*., 2021). Compared to the traditional approach, advancements in remote sensing technology offer opportunities for mapping palatable grass biomass over large geographic areas. This technology has proven to be successful and effective in estimating vegetation biomass, offering a time- and cost-efficient alternative in estimating and mapping palatable grass biomass as an indicator of rangeland quality. Evaluation of vegetation parameters using remote sensing instruments (that collect spectral reflectance measurements) has previously been conducted by satellites and aircraft (Nasi *et al*., 2018; Théau *et al*., 2021).

The PlanetScope and Unmanned Aerial Vehicles (UAV) are among the remote sensing sensors utilised in mapping the palatable grass biomass in communal rangelands. The Planet Labs-operated PlanetScope is a new generation of satellites characterised by constellation of satellites, known as CubeSats which are in a sun-synchronous orbit with an equator crossing time between 9:30 and 11:30 (local solar time) (Planet Labs Inc, 2023). It provides high spatial resolution of 3 m multispectral data, rapid and continuous coverage of the Earth's surface. These satellites are commercial CubeSats, which are quickly emerging as essential tools for mapping the Earth's surface (Frazier and Hemingway, 2021). New technological advancements, such as the lightweight multi- and hyper-spectral sensors, carried by drones or Unmanned Aerial Vehicles (UAV), have become widely available in recent years (Nasi *et al*., 2018). UAVs offer new alternatives to traditional remote sensing technologies. The newly advanced use of drone-based photogrammetric 3D data has been promising for biomass evaluation; furthermore, combining the 3D data and spectral data has improved the results (Viljanen *et a*l., 2018).

Although remote sensing offers the potential to increase the scope of palatable grass biomass mapping, there are several statistical approaches for mapping palatable grass biomass, with each having its own strengths and weaknesses. The application of linear regression models and non-linear regression models for palatable grass biomass has been implemented by using various predictor variables such as spectral vegetation indices retrieved from satellite imagery. Remote sensing data can be used to generate variables such as multispectral bands, vegetation indices, and textural measurements which are suited for rangeland investigations (Gruner *et al*., 2020; Sharifi and Felegari, 2023). Myriad studies have utilised vegetation indices (VIs) adopted for multispectral or hyperspectral data. A primary vegetation index (VIs) such as the Normalised Difference Vegetation Index (NDVI) is a commonly used index that uses spectral reflectance data to determine the vegetation greenness and density and has often been used to evaluate the palatable grass biomass. In combination with spectral bands and vegetation indices, texture measurements have also been used in mapping palatable grass biomass. The Gray-level

© University of Venda

co-occurrence matrix (GLCM) texture metrics provide useful insights into colour and structural patterns within a landscape by extracting spatial data such as canopy roughness (Iqbal *et al*., 2021).

Several studies have conducted regression analysis in mapping grass biomass. A study by Clementini *et al*., (2020) has successfully evaluated long-term grass biomass estimation in an African region. In their studies, (Hunt et *al*., 2003; Svinurai *et al*., 2021) have both worked on mapping grass biomass while focusing on the use of linear regression models. Another study by (Tapamo *et al*., 2014) compared the linear and non-linear models, such as Principal component analysis (PCA), with classification techniques for estimating forest biomass from texture analysis and established that non-linear classification models, such as SVM and random forests could improve prediction accuracy and precision. About 64 research studies that have used UAVs in estimating biomass have been reviewed by (Bazzo *et al*., 2023). Even though no comparison was made with non-linear models for accuracy, his study found linear regression to be the most popular model used. A range of studies have evaluated the performance of linear and non-linear regression models for mapping the quality of biomass, yet a few studies have systematically compared linear versus no-linear regression models in mapping the quality of biomass. Thus, the objectives of this study were to (i) Compare the performance of linear and non-linear models for estimating palatable grass biomass using PlanetScope data and (ii) to compare the performance of linear and non-linear models for estimating palatable grass biomass using UAV data and PlanetScope subset data. The rangelands surrounding rural villages are heavily reliant on livestock grazing for livelihoods. Therefore, accurate and reliable mapping of palatable grass biomass is critical for sustainable land use and resource management.

3.3 Methods and Materials

3.3.1 Study Area

The research study area is situated in the Collins Chabane Local Municipality (CCLM). This local municipality lies within the Vhembe District Municipality in the far north of the Limpopo Province of South Africa. The Municipality is one of the four local municipalities in the district and makes up 20% of its geographical area with a jurisdiction area covering 5 467.216km² (22° 35′ S and 30° 40′ E). A single study site selected for the purpose of testing the utility of both PS and UAV data. **Figure 3.1** (a) depicts the first study site chosen as the primary site and within this larger site, a subset was delineated as the second study site presented in **Figure 3.1** (b). The unemployment rate in this area was reported to be 45% in 2021 (Murei *et al*., 2022), which leads to communities within the area being highly dependent on their communal land for cattle grazing, which contributes to their livelihoods (Sikhweni and Hassan, 2014a) Subsistence farming,

© University of Venda

raising animals, and human settlement are the principal land uses in the region (Chamunika *et al*., 2014; Sikhweni and Hassan, 2014b). The site is characterised by conversion of croplands to grazing areas and the open lands and farms are used by livestock farmers as grazing lands.

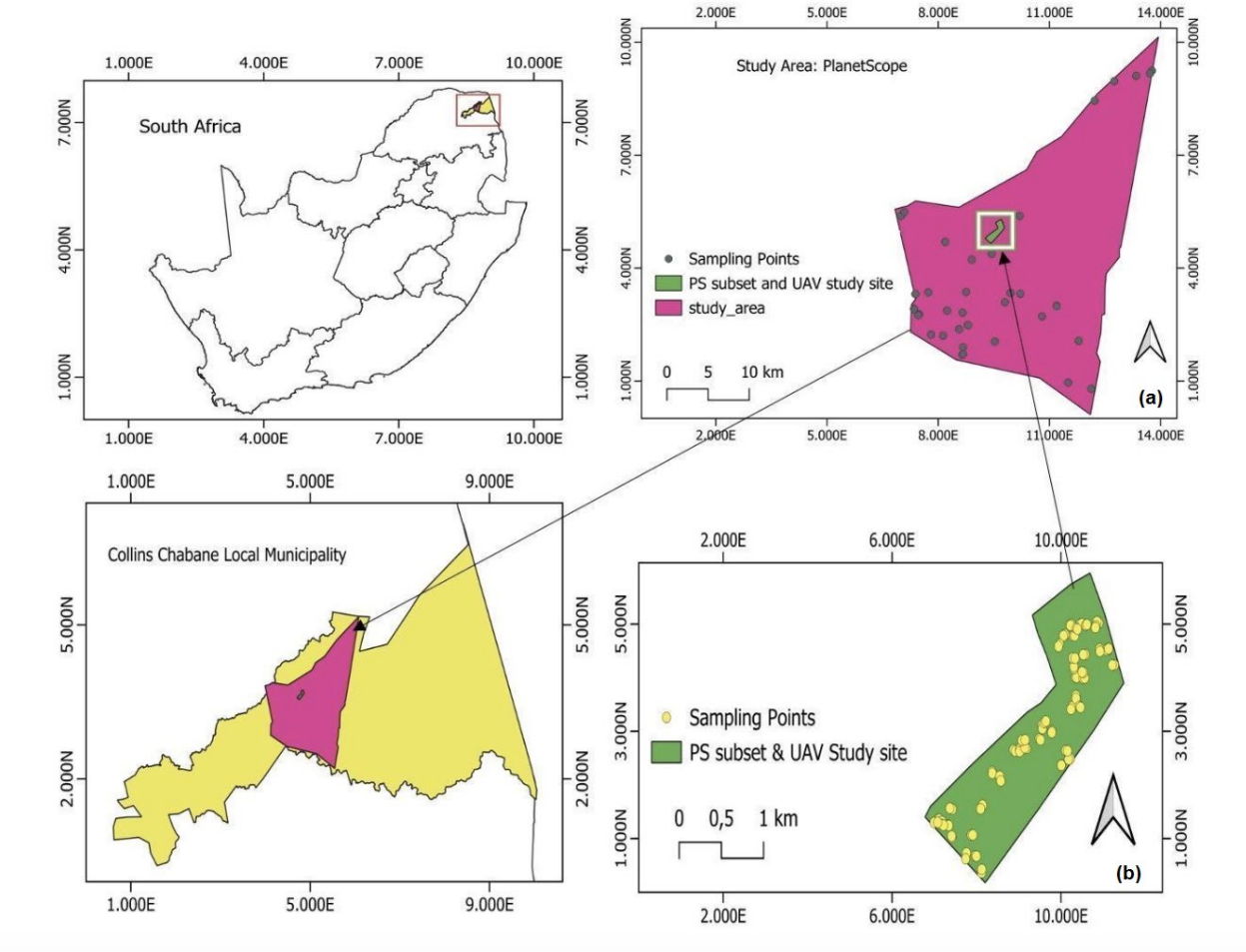


Figure 3.1: Location of the study area and distribution of field survey points for both study sites. The first study site (a) was for the PlanetScope primary site, and the second study site was for the PlanetScope subset site and UAV site.

3.3.2 Field Data Collection

The field data collections were conducted between September and October 2022 for the first study site and between March and April 2023 for the second study site. Field data collection consists of different dates by reason of logistical limitations that hindered surveying the entire study area at once and also to address the study's objectives thereby

© University of Venda

ensure comprehensive coverage with robust analysis. The first dataset (September and October 2022) was utilised to evaluate model's performance with the use of the PlanetScope data, while the second dataset focused on comparison between the UAV and PlanetScope sub-set data. During the fieldwork, sampling areas measuring 30m × 30m were randomly established. Within each of these areas, two plots were randomly selected by placing a 5m × 5m square wire frame on the field. Thus, resulting in sub-plots measuring 0.5 × 0.5m. Palatable grass species were observed within the sample points and calculated against unpalatable grass species. The samples were then manually harvested within the 5m × 5m sub-plots. After harvesting the grass species, the wet biomass was weighted in the field using a kitchen scale, recorded, and stored in sample bags. The samples were later oven dried at 70°C in the laboratory for 24 hours to obtain the dry mass (g/m^2) values. The spatial distribution of the sampling points is shown in **Figure 3.1**. A handheld standard Garmin eTrex 20™ Global Positioning System (GPS) device was employed to record the coordinates of the points with a maximum accuracy of 3 m. The standard sample dataset of n = 172 grass samples was divided into 70% (n = 120) for training the predictive model and 30% (n = 52) for validating the predictive model. The vegetation coverage was visually estimated within the 30 m and 0.5 m points per sample area with an average of 63,25% cover within 30 m and 73,81% cover within the 0.5 m sample area. The grass species prevalent in the sampled plots include: *Urochloa panicoides*, *Urochloa mosambicensis*, *Themeda triandra*, *Sporobolus africanus*, *Digitaria sanguinalis*, *Cynodon dactylon*, *Panicum maximum*, which were palatable grass species and *Heteropogon contortus* was found to be unpalatable species within the sampled plots.

3.3.3 Remote Sensing Techniques

3.3.3.1 PlanetScope data

PlanetScope imagery was selected as the data source for this study because of its high spatial resolution and short revisit time (Sikhweni and Hassan, 2014b). The PS imagery with a 3 m spatial resolution is a CubeSat multispectral cloud-free image covering the study area acquired on the 1st of October 2022 from Planet Labs. The PS sensors acquire spectral imagery in four spectral bands: blue (455–515 nm), green (500–590 nm), red (590–670 nm), and near infrared (NIR) (780–860 nm) (Dos Reis *et al*., 2020). The imagery employed was Planet Labs' atmospherically corrected Level-3B surface reflectance products. Images obtained were merged into a mosaic for subsequent analytical purposes in Quantum GIS (version 3.28.3) software (QGIS Development Team, 2022). The coordinates of the sampled points were used to extract pixel values of the PS imagery. This was done to generate the values of the predictor variables (such as vegetation indices) for model development.

© University of Venda

3.3.3.2 UAV data

Alongside the PS data, UAV imagery was used to obtain high-resolution spatial data of 0.3 m. Remote sensing applications have advanced to fine scales with the emergence of this platform (Maimaitijiang *et al*., 2020). The data collection was outsourced to a professional aerial data services provider called DPS Aerial Surveys. The DPS Aerial Surveys conducted UAV flights with the use of drones flown across the study area at an altitude of 30 m. The UAV image acquisition was conducted on December the 6th, 2022. Like the satellite data, a pre-processed RGB final product was obtained from the company. The data was acquired through their skilled services to align with the necessary specifications required for the study.

3.3.3.3 PlanetScope Subset data

From the PlanetScope primary imagery, a specific region of interest was extracted to obtain UAV and subset imagery. Due to the fact that the UAV drone could not cover the entire study area, only a portion of the study area could be utilised, hence, the strategic carving of the UAV data from the primary study area. The subset image was then created from the spatial boundaries obtained from the UAV shapefile. This then became the smaller-scale version of the larger PlanetScope image. This approach was aimed at extracting and focusing on a part that corresponds to the acquisition of UAV data to ensure a homogeneous vegetation distribution thereby enabling detailed comparison and integration of high-resolution UAV with PlanetScope subset data.

3.3.4 Predictor Variable Selection and Extraction

The predictor variables have been widely used in remote sensing for numerous studies. A selection of predictor variables was utilised in the study to predict palatable grass biomass for mapping purposes. Three categorical variables explored in the study were spectral bands, spectral indices, and GLCM features, which were derived from both the PS imagery and the UAV imagery. The selection of the three sets of variables was applied because of their ability to capture key characteristics such as spectral reflectance, indices, and textural features (Svinurai, 2021; Dobrinić *et al*., 2022; Mohammadpour *et al*., 2022). The first set of predictors comprises the spectral bands with reflectance characteristics together with specific spectral signatures corresponding to palatable grass biomass (Svinurai, 2020). The study utilised the four bands - red, blue, green, and NIR from the PlanetScope bands and the UAV three RGB (red, green, and blue) bands.

The second set was the vegetation indices that are computed from spectral bands serving as representatives of environmental factors like grass health, chlorophyll content, and soil

© University of Venda

moisture. The derived Spectral indices from the PlanetScope imageries were: Normalised Difference Vegetation Index (NDVI), Normalised Difference Water Index (NDWI), Visible Atmospheric Resistant Index (VARI), Enhanced Vegetation Index (EVI), Green Normalised Difference Vegetation Index (GNDVI), Soil-Adjusted Vegetation Index (SAVI), Simple Ratio 1 (SR1B), Simple Ratio 2 (SR2G) and Simple Ratio 3 (SR3R) (**Table 3.1**). The Visible Atmospheric Resistant Index (VARI), Green-Red Vegetation Index (GRVI), Red-Green-Blue Vegetation Index (RGBVI), Green Leaf Index (GLI), Brightness Index (BI), Soil Composition Index (SCI), Visible-band Difference Vegetation Index (VIDVI), Modified Green-Red Vegetation Index (MGVRI), Green Chromatic Coordinate (GCC), Red Chromatic Coordinate (RCC), Blue Chromatic coordinate (BCC), Normalised Red-blue Difference Index (NRBDI), Normalised Green-Blue Difference Index (NGBDI), Green-Blue Vegetation Index (GBVI), Red-Green-Blue Ratio Index (RGBRI) were all derived from the UAV imagery for palatable grass biomass mapping (**Table 3.2**). The use of vegetation indices in mapping palatable grass biomass is a well-established technique used in numerous studies. In their study (Dos Reis *et al*., 2020) evaluated the potential of spectral bands, spectral indices, and texture measures obtained from PS imagery in mapping pasture biomass and canopy height (CH).
The results showed improved estimation in biomass and CH with the integration of texture measure as compared to the utilisation of the spectral bands or vegetation indices only. A study by (Corti *et al*., 2023) integrated crop height with vegetation indices and the fraction of soil covered by the crops to enhance the biomass estimation of herbaceous crops. The selection of these indices was influenced by the correlation with the grass biomass (Adam *et al*., 2010). The indices were calculated within Microsoft Excel with the use of a statistical combination of spectral bands from both the PlanetScope data and UAV data.

The study also employed the use of textural data which were GLCM measures derived from both the PlanetScope data and the UAV data. The GLCM matrix is a widely used technique developed by (Haralick *et al*., 1973). Textural measures offer valuable insights into palatable grass biomass through spatial distribution quantification. The GLCM texture features employed include Contrast, Dissimilarity, Homogeneity, Angular Second Moment, Energy, Maximum Probability, Mean, Variance, Entropy, and Correlation (**Table 3.1 & 3.2**). Previous studies have already revealed the effectiveness of GLCM features in mapping palatable grass biomass (Li *et al*., 2021; Mohammadpour et al., 2022). The study utilised a 5 × 5 moving window with 32 quantization levels, a probabilistic quantizer, at an offset distance of 1 pixel in all directions (0°,35°,90° and 135°). Texture images were extracted by using the GLCM statistical texture approach within the Sentinel Application tool (SNAP) version 9.0.0 (European Space Agency, 2022). A total of 10 texture features were generated for each PlanetScope image and 10 for the

© University of Venda

UAV image. The images of each textural feature were used to retrieve the feature values from the coordinates of the sampling points using the QGIS Software for later use in model development.

Table 3.1: Description and formula of selected variables, including raw bands, vegetation indices, and texture features, derived from PlanetScope imagery for mapping palatable grass biomass in this study.

Feature categories	Feature Names	Details	References
Bands	Blue (B)	455-515nm	(Dos Reis *et al.*, 2020)
	Green (G)	500-590nm	
	Red (R)	590-670nm	
	Near-Infrared (NIR)	780-860nm	
Vegetation Indices	Normalised Difference Vegetation Index (NDVI)	$(NIR - R) / (NIR + R)$	(Rouse *et al.*, 1974)
	Normalised Difference Water Index (NDWI)	$(G - NIR) / (G + NIR)$	(Jovanovic *et al.*, 2014)
	Visible Atmospheric Resistant Index (VARI)	$(G - R) / (G + R - B)$	(Erunova *et al.*, 2021)
	Enhanced Vegetation Index (EVI)	$(2.5 (NIR - G)) / (NIR + (6 \times R) + (7.5 \times B) + 1)$	(Xue and Su, 2017)
	Green Normalised Difference Vegetation Index (GNDVI)	$(NIR - G) / (NIR + G)$	(Gitelson *et al.*, 1996)
	Soil-Adjusted Vegetation Index (SAVI)	$\left(\frac{(NIR - R)}{(NIR + R + 0.5)} \times (1 + 0.5)\right)$	(Huete, 1988)
	Simple Ratio 1 (SR1B)	NIR / B	(Romero *et al.*, 2018)
	Simple Ratio 2 (SR2G)	NIR / G	
	Simple Ratio 3 (SR3R)	NIR / R	
Gray-level co-occurrence matrices (GLCM)	Contrast	$\sum_{i,j=0}^{N-1} iP_{i,j}$	(Li *et al.*, 2021)
	Dissimilarity	$\sum_{i,j=0}^{N-1} iP_{i,j} \lvert i - j \rvert$	(Li *et al.*, 2021)
	Homogeneity	$\sum_{i,j=0}^{N-1} iP_{i,j} / (1 + (i - j)^2)$	(Li *et al.*, 2021)
	Angular Second Moment	$\sum_{i,j=0}^{N-1} iP_{i,j}\ 2$	(Li *et al.*, 2021)
	Energy	$Energy = \sqrt{ASM}$	(Hall-Beyer, 2017)
	Maximum Probability	$Maximum\ Probability = (\rho(i,j))$	(Amadasun and King, 1989)
	Mean	$\sum_{i,j=0}^{N-1} iP_{i,j}$	(Li *et al.*, 2021)
	Variance	$\sum_{i,j=0}^{N-1} iP_{i,j} (1 - \mu_i)$	(Li *et al.*, 2021)

© University of Venda

	Entropy Correlation	$\sum_{i,j=0}^{N-1} iP_{i,j}\, ln\, P_{i,j}$ $\sum_{i,j=0}^{N-1} \left(\frac{i(\sum_{i,j}^{N-1} ijiP_{i,j-}\, \mu i\mu i)}{0_i^2 0_j^2}\right)$	(Li *et al.*, 2021)

Table 3.2: Description and formula of selected variables, including raw bands, vegetation indices, and texture features, derived from UAV imagery for mapping palatable grass biomass in this study.

Feature categories	Feature Names	Details	References
Bands	Red (R) Green (G) Blue (B)	0.6 – 0.7 µm 0.5 – 0.6 µm 0.4 – 0.5 µm	\
Vegetation Indices	Visible Atmospheric Resistant Index (VARI)	$(G - R) / (G + R - B)$	(Gitelson *et al.*, 1996)
	Green-Red Vegetation Index (GRVI)	$(G - R) / (G + R)$	(Falkowski *et al.*, 2005; Tucker, 1979; Bendig *et al.*, 2015)
	Red-Green-Blue Vegetation Index (RGBVI)	$(G^2 - B \times R) / (G^2 + B \times R)$	
	Green Leaf Index (GLI)	$(G - R) + (G - B) / (2G + R + B)$	(Eng *et al.*, 2019)
	Brightness Index (BI)	$\sqrt{(R \times 2) + (G \times 2) + (B \times 2) / 3}$	(Marques *et al.*, 2020)
	Soil Composition Index (SCI)	$(R - G) / (R + G)$	(Serbin *et al.*, 2009)
	Visible-band Difference Vegetation Index (VIDVI)	$(2G - R) / (G + R - B)$	(Xue and Su, 2017)
	Modified Green-Red Vegetation Index (MGVRI)	$(G)^2 - (R)^2 / (G)^2 + (R)^2$	(Bendig *et al.*, 2015)
	Green Chromatic Coordinate (GCC)	$G / (R + G + B)$	(O'Connell and Alber, 2016)
	Red Chromatic Coordinate (RCC)	$R / (R + G + B)$	(O'Connell and Alber, 2016)
	Blue Chromatic coordinate (BCC)	$B / (R + G + B)$	(O'Connell and Alber, 2016)
	Normalised Red-blue Difference Index (NRBDI)	$(R - B) / (R + B)$	(Gitelson *et al.*, 2002)
	Normalised Green-Blue Difference Index (NGBDI)	$(G - B) / (G + B)$	(Zhang *et al.*, 2023)
	Red-Green-Blue Ratio Index (RGBRI)	$(R + B) / 2G$	(Zhang *et al.*, 2023)
Gray-level co-occurrence matrices (GLCM)	Contrast	$\sum_{i,j=0}^{N-1} iP_{i,j}$	(Li *et al.*, 2021)
	Dissimilarity	$\sum_{i,j=0}^{N-1} iP_{i,j} \lvert i - j \rvert$	(Li *et al.*, 2021)
	Homogeneity	$\sum_{i,j=0}^{N-1} iP_{i,j} / (1 + (i - j)^2)$	(Li *et al.*, 2021)
	Angular Second Moment	$\sum_{i,j=0}^{N-1} iP_{i,j}\, 2$	(Li *et al.*, 2021)
	Energy	$Energy = \sqrt{ASM}$	(Hall-Beyer, 2017)

© University of Venda

	Maximum Probability	$Maximum\ Probability = (\rho(i,j))$	(Amadasun and King, 1989)
	Mean	$\sum_{i,j=0}^{N-1} iP_{i,j}$	(Li *et al.*, 2021)
	Variance	$\sum_{i,j=0}^{N-1} iP_{i,j}\,(1 - \mu_i)$	(Li *et al.*, 2021)
	Entropy	$\sum_{i,j=0}^{N-1} iP_{i,j}\,ln\,P_{i,j}$	(Li *et al.*, 2021)
	Correlation	$\sum_{i,j=0}^{N-1}\left(\frac{i(\sum_{i,j}^{N-1} ijiP_{i,j-}\mu i\mu i)}{0_i^2 0_j^2}\right)$	(Li *et al.*, 2021)

3.3.5 Construction of palatable grass biomass evaluation models

Regression techniques emerge as powerful tools in producing accurate and precise maps, and they serve as predictive models while utilising predictor variables generated from remote sensing data. The performance of different models in mapping palatable grass biomass can be assessed by employing both Linear regression and non-linear regression (with an exponential function) models. The use of a linear regression model is effective yet straightforward in evaluating palatable grass biomass (Nakano *et al.*, 2020; Quang *et al.*, 2022). Linear regression fits a linear equation to the observed data with the aim of predicting the relationship between the predictor variables and the response variable. On the other hand, non-linear regression assumes a non-linear relationship between the response and predictor variables. The study employed a total of 24 models. Although referred to as linear regression, in the context of this study, the multiple linear regression was utilised as the modelling approach and it employed multiple independent variables. In this case, the formula is given as:

$$y = \beta_0 + \beta_1 x_1 + \beta_2 x_2 + \cdots + \beta_i x_i \quad (1)$$

where y is the dependent variable, x_1, x_2 … x_i are the independent variables, β_0 is the y-intercept and β_i is the regression coefficient representing the change in y with respect to the change in x_i.

The non-linear (Exponential) model is given off by the equation:

$$y = \beta_0 + \beta_1 log\,(x_1) + \beta_2 log\,(x_2) + \cdots + \beta_i log\,(x_i) \quad (2)$$

© University of Venda

where y is the dependent variable, $log\ log\ (x_1)$,$log\ log\ (x_2)$ ... $log\ log\ (x_i)$ represent the natural logarithms of the independent variables, β_0 is the y-intercept and β_i is the regression coefficient representing the change in y with respect to the change in $log\ log\ (x_i)$.

The remote sensing datasets were split into 70% used for model training and 30% which was reserved for model validation. In the initial phase, with the use of the PlanetScope large data, multiple linear regression models were computed by using various attributes. The first model to be computed was done by making use of spectral bands only. This enabled the assessment of the linear relationship between palatable grass biomass and the bands. Secondly, only the vegetation indices derived from the PlanetScope bands were employed for the model. Thirdly, GLCM features were used for the model computation. Lastly, to evaluate the combined impact of these predictor variables on grass biomass estimation, the linear model was developed by combining all the bands, indices, and GLCM measures. The combination of these features aids the model to capture a broader range of factors influencing palatable grass biomass. After the combined model fitting, a backward stepwise regression was conducted using the "step()" function within the R programming software (version 4.2) (R Core Team, 2022). This was done to encourage a confined and applicable model by removing less significant predictors for estimating palatable grass biomass so long as the reduction enhanced the model (Kelsey and Neff, 2014). All four regression models were compared to obtain the optimal linear regression model for estimating palatable grass biomass with the PlanetScope large data. Apart from the linear relationship, the study also applied non-linear regression models by computing bands, indices, GLCM, and the combination of all features, much like the linear technique did. The models were conducted by applying the natural logarithm transformation using the "log()" function (on the predictor variables) (Zach, 2021) within the R programming software (version 4.2) (R Core Team, 2022). The "lm()" function was applied to fit the exponential regression model while using the transformed predictor variables as input variables for the "lm()" function. Likewise, all four regression models were compared to obtain the optimal linear regression model for estimating palatable grass biomass with the PlanetScope subset data and UAV data.

By implementing the same consecutive technique performed for the PlanetScope large data, the linear regression and non-linear regression models were constructed for bands, indices, GLCM, and combined feature model for the performance comparison of the

© University of Venda

linear and non-linear models for estimating palatable grass biomass between the UAV data and PlanetScope subset data. Likewise, all regression models were compared to obtain the optimal linear regression and non-linear regression model for estimating palatable grass biomass within firstly, the PlanetScope subset data and, secondly, the UAV data. The R programming software (version 4.2) (R Core Team, 2022) was adopted for all statistical analysis. The coefficient of determination (R^2) and the P-value of each model output were used for the comparison and obtaining the ideal model with each model subcategory. The two metrics offer valuable insights on how well the model fits the data and the model's predictive power, while guiding on the selection of the most suitable approach for effective palatable grass biomass mapping. The model that obtained the highest (R^2) and lowest *p*-value between the linear and non-linear regression model of the PlanetScope large data was selected for use in the predictive mapping of the grass biomass. This selection process was conducted in the same manner for the comparison between the UAV data and the PlanetScope subset data. Comparing different models is helpful for revealing the relationships between palatable grass biomass and the Remote Sensing variables.

3.3.6 Assessing Model Accuracy

The performance of the optimal models within all the datasets were selected based on the model fit metrics from the training dataset, which is the R-squared and the *p*-value. The accuracy of the final models was then quantified based on three standard statistical measures, namely the root mean squared error (RMSE), mean absolute error (MAE), and lastly, the coefficient of determination (R^2) with the use of the 30% validation. Model accuracy assessment is an essential procedure as it highlights how well the model has performed in its predictions (Owusu-Adjei *et al*., 2023). Regression analysis often employs the RMSE, MAE, and R^2 in evaluating the predictive capability and model performance, offering the opportunity to assess its accuracy and reliability. RMSE (equation 3) indicates an error metric which measures the difference between the predicted value and the observed value. The MAE (equation 4) shows the average value of the absolute errors between the predicted and measured values. R^2 (equation 5) determines the proportion of variance in the dependent variable that can be explained by the independent variables. Its range is from 0 to 1, where a higher value indicates a better model fit to the data.

The above metrics can be expressed as,

© University of Venda

$$RMSE = \frac{1}{n}\sum_{i=1}^{n}\left(Y_i - \hat{Y}_1\right)^2 \quad (3)$$

$$MAE = \frac{1}{n}\sum_{i=1}^{n}\left|Y_i - \hat{Y}_1\right| \quad (4)$$

$$R^2 = 1 - \frac{SS_{RES}}{SS_{TOT}} = 1 - \frac{\sum_{i=1}^{n}(Y_i - Y_1)^2}{\sum_{i=1}^{n}\left(Y_i - \underline{y}\right)^2} \quad (5)$$

where $\hat{Y}_1$ is the predicted value, Y_i is the observed value and n the total number of the validation observations. Where SS_{RES} is the sum of squares due to regression (explained sum of squares), and SS_{TOT} is the total sum of squared errors (Chicco *et al*., 2021; Tatachar, 2021; Zhou *et al*., 2023).

3.4 Results

The study tested different models for the purpose of comparison analysis (1) between the Linear and non-linear regression model derived from PlanetScope data in mapping palatable grass biomass, and (2) performance comparison of linear and non-linear regression models between the UAV data and PlanetScope subset data for palatable grass biomass mapping.

3.4.1 Comparison of Linear and non-linear regression models derived from PlanetScope data.

The study compared the performance of the linear and non-linear regression models derived from the PlanetScope data to determine which models were better suited for mapping palatable grass biomass. The combination of the bands, indices, and GLCM features in the model showed improved performance within the linear model as compared to using bands, indices, or GLCM features independently. On the other hand, the exponential model with all features combined emerged as the most significant model for estimating palatable grass biomass when compared to the use of the other variable features on their own. The exponential model with all combined features achieved the highest R^2 value of 0.45 and the lowest *p*-value of 0.0016, suggesting a robust predictive power for mapping biomass in contrast to the best linear regression model also with the

© University of Venda

use of combined features that achieved an R^2 value and *p*-value of 0.22 and 0.023, respectively. The results from the PlanetScope primary imagery from both the linear models and the exponential models have shown that the use of bands, indices and GLCM measures separately does not show any efficiency, but as soon as the use of all combined features is introduced, the model showed improvement in the predictions with the exponential model outcompeting the linear regression model. The bar graph in **Figure 3.2** is indicative of how the two models, with respect to the predictor variables, have performed while providing insights into their respective strengths and weaknesses in mapping palatable grass biomass. The figure clearly shows the exponential model's superior performance with the combined predictor variables. **Table 3.3** shows the results obtained from all the models computed for both the linear and non-linear regression models. The results obtained from the PlanetScope image, however, were insufficient in the mapping processes of the palatable grass biomass.

Table 3.3: The initial results obtained from the PlanetScope primary image for both the Linear model and Exponential model.

Model Type	Data source	Feature type	R^2	*p*-value
Linear Models:	PlanetScope	Bands	0.08	0.23
		Indices	0.12	0.04
		GLCM	0.08	0.13
		Combined	0.22	0.02
Exponential Models:		Bands	0.05	0.33
		Indices	0.16	0.04
		GLCM	0.22	0.04
		Combined	0.45	0.00

© University of Venda

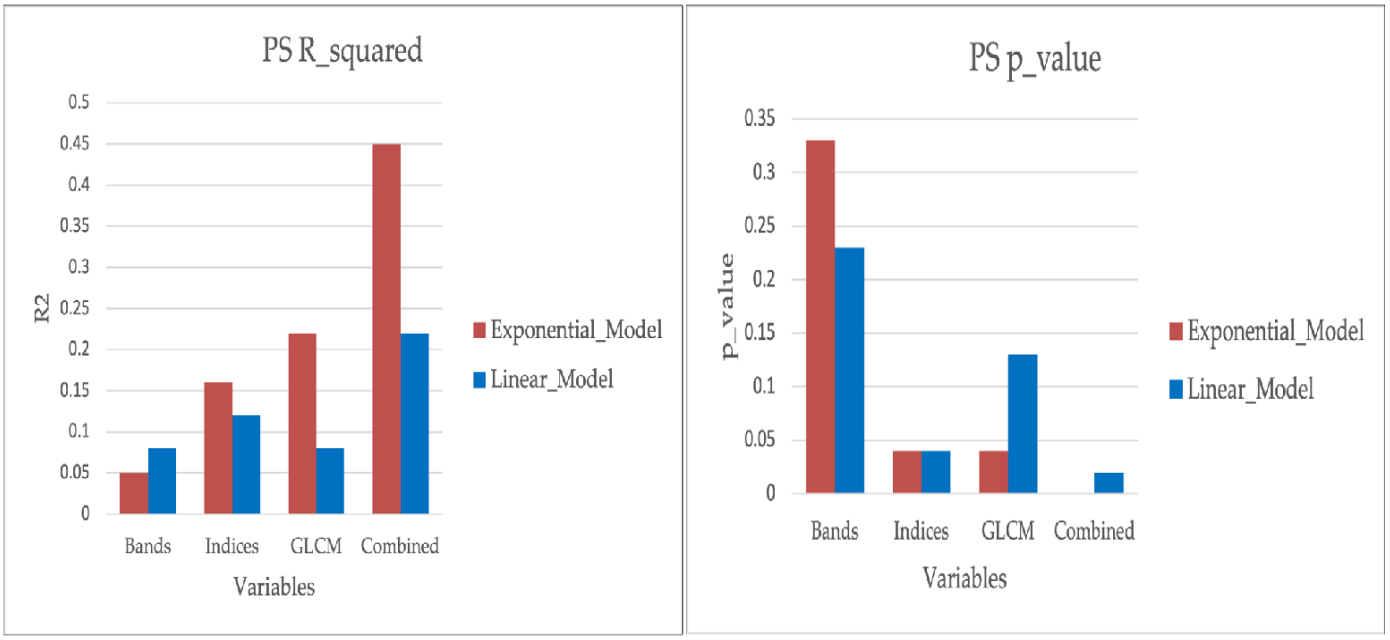


Figure 3.2: Comparison of Linear and Non-Linear (Exponential) Models on PlanetScope Data with the use of Indices, Bands, and GLCM Measures as predictor variables as computed from the initial model.

The study was then computed and tested the variables obtained from the PlanetScope subset final model to determine its capability in generating a palatable grass biomass map. The model included a combination of spectral indices and GLCM features, NDVI, EVI, SAVI and Variance (**Table 3.4**). These variables showed the strongest predictive relationship with palatable grass biomass.

Table 3.4: The results obtained from the final linear model used for mapping palatable grass biomass, with the validation metrics utilised to access model accuracy.

Predictor	Estimates	Std. Error	*z* value	*p* value
(Intercept)	2.477e+01	1.036e+01	2.39	0.021 *
NDVI	-3.035e+04	2.315e+04	-1.31	0.197
EVI	1.302e+02	1.190e+02	1.09	0.280
SAVI	2.015e+04	1.543e+04	1.31	0.198

© University of Venda

Variance	-1.855e-03	5.562e-03	-0.33	0.740
Significant levels: 0'*' 0.001'**' 0.01'*' 0.05'.' 0.1' '1** **Multiple R-squared: 0.11** ***p*-value: 0.25**				

Figure 3.3 illustrates the palatable grass biomass map produced from the PlanetScope big imagery. The map visually represents the spatial distribution of palatable grass biomass within the study area with distinct colours on the map corresponding to the estimated value of the biomass the study area holds. The high biomass areas and low palatable grass biomass areas are depicted with distinct colours and their corresponding values with the value of 73.07 for high biomass and 0 for the lowest/no biomass distribution in the study.

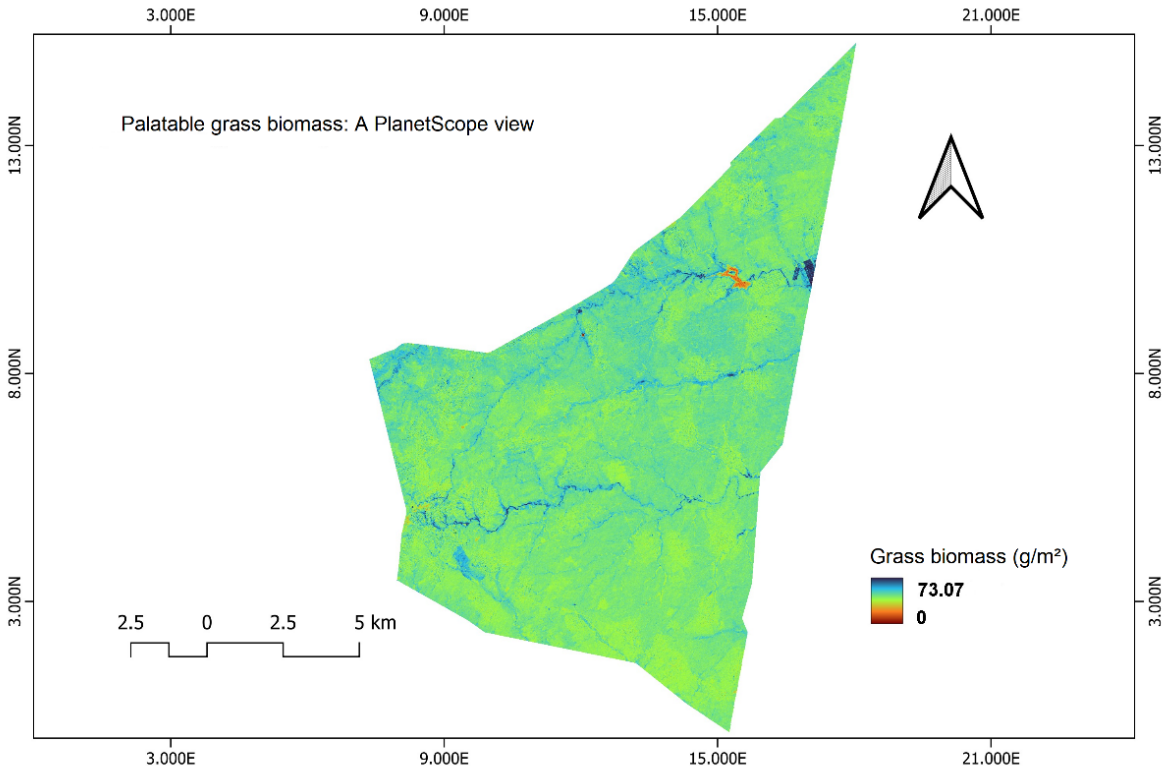


Figure 3.3: Palatable grass biomass spatial map as predicted by the Linear regression model derived from the PlanetScope big image.

© University of Venda

Figure 3.4 depicts the observed versus the predicted palatable grass biomass. The visual representation provides insights into the performance of the predictive model in capturing the observed trends in palatable grass biomass. The scatter plot reveals predictions from the model not aligning closely with the observed data resulting in a not so strong relationship between the observed and the predicted biomass values. An overestimation of palatable grass biomass values for lower observed values and an underestimation of palatable grass biomass values for higher observed values is revealed with the scatterplot.

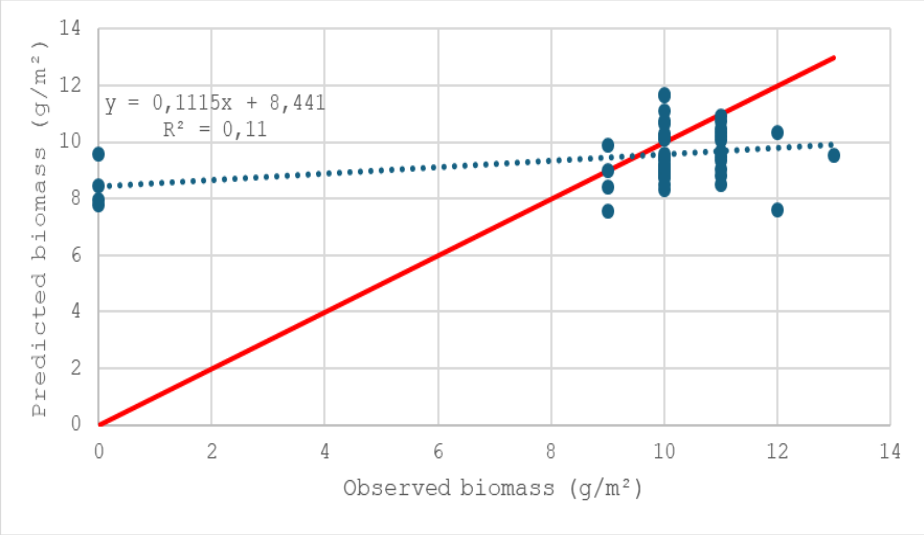


Figure 3.4: Scatterplot of the measured vs. predicted palatable grass biomass, g/m²) by linear regression model from PlanetScope big image. A red line is provided as a reference line.

The model obtained an RMSE of 2.16, MAE of 1.69 and R^2 of 0.11 (**Table 3.5**).

Table 3.5: Obtained validation metrics values from the PlanetScope big image.

Validation			
Data source	**RMSE**	**MAE**	**R^2**
PlanetScope big image	2.16	1.69	0.11

RMSE = root mean squared Error, MAE = mean absolute error, R^2 = Coefficient of determination.

© University of Venda

3.4.2 Performance comparison of linear and non-linear models between the UAV data and PlanetScope subset data.

The study further compared the performance of the linear and non-linear regression models between the UAV data and PlanetScope subset data to determine best remote sensing data for mapping palatable grass biomass. The model results obtained from both the subset image and the UAV imagery are displayed in **Table 3.6.**

3.4.2.1 Optimal PlanetScope subset model

Upon conducting model evaluation and comparison between the linear regression and exponential regression model derived from the PlanetScope subset imagery, the results displayed the linear model with all combined features as the optimal models for palatable grass biomass mapping (**Table 3.6**).

Table 3.6: Initial results obtained for both the PlanetScope subset and UAV data.

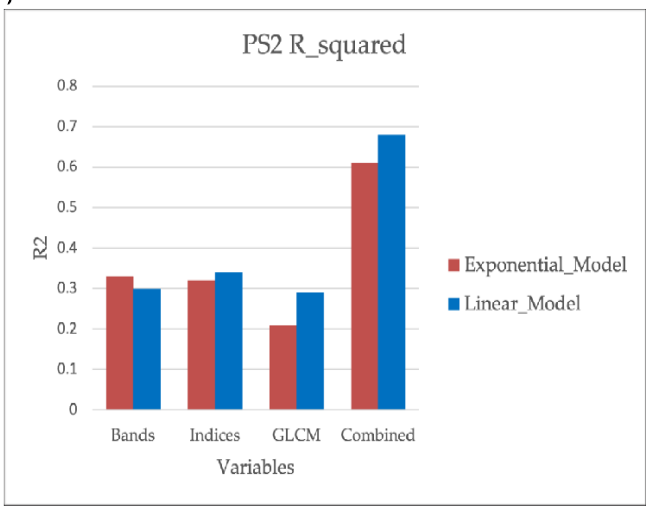
Model Type	Data source	Feature type	R^2	R^2(%)	*p*-value
Linear Models:	PS Subset	Bands	0.03	30%	0.003
		Indices	0.34	34%	0.0002
		GLCM	0.29	30%	0.007
		Combined	0.68	68%	0.0004
	UAV	Bands	0.03	3%	0.746
		Indices	0.15	15%	0.213
		GLCM	0.13	13%	0.799
		Combined	0.28	28%	0.073
Exponential Models:	PS Subset	Bands	0.33	33%	0.001
		Indices	0.32	31%	0.0006
		GLCM	0.21	21%	0.074
		Combined	0.61	61%	0.0002
		Bands	0.02	2%	0.713

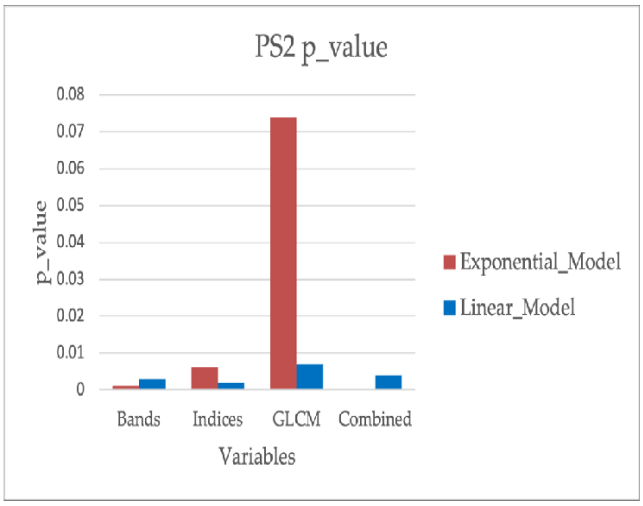
© University of Venda

	UAV	Indices	0.02	2%	0.922
		GLCM	0.06	7%	0.272
		Combined	0.18	18%	0.876

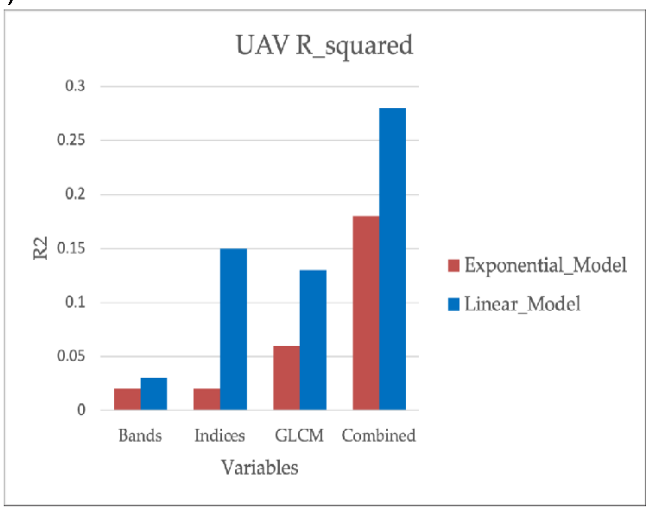
The bar-graph in **figure 3.5** illustrates how the two models from their PlanetScope data (a) and the UAV data (b) with respect to the predictor variables have performed and provide useful insights on the predictor's strength and weaknesses in mapping palatable grass biomass. From the PlanetScope subset image we can clearly see that the combined linear regression model outcompetes the use of the other variables while used separately and the linear regression model with the combined variables highlights its superior performance over the other variables.

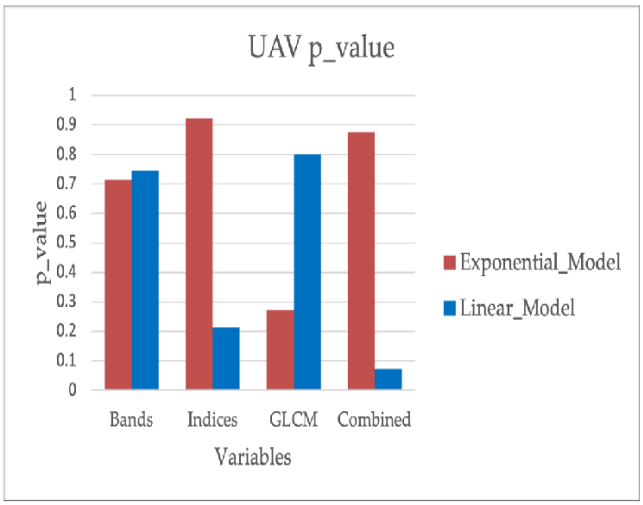
a)





b)





© University of Venda

Figure 3.5: Comparison of Linear and Non-Linear (Exponential) Models on PlanetScope subset data (a) and UAV data (b) with the use Indices, Bands, and GLCM Measures as predictor variables as computed from the initial model.

Nonetheless, for the purpose of mapping, the results obtained from the model were inadequate. The best regression model was then obtained via forward and backward stepwise regression and resulted in predictor variables including NDVI, EVI, SAVI, and Variance. The model achieved the R^2 value of 0.33 and the *p*-value of 0.0006 (**Table 3.7**). This suggests that the predictor variables had strong positive associations with the palatable grass biomass.

Table 3.7: The results obtained from the final linear model used for mapping palatable grass biomass derived from PlanetScope subset image, with the validation metrics used to assess model accuracy.

PlanetScope subset imagery				
Predictor	**Estimates**	**Std. Error**	***z* value**	***p* value**
(Intercept)	-1.603e+01	1.269e+01	-1.264	0.21282
NDVI	6.514e+05	2.142e+05	3.041	0.00393**
EVI	1.119e+02	7.999e+01	1.399	0.16873
SAVI	-4.344+05	1.429e+05	-3.040	0.00393**
Variance	7.458e-3	3.904e-03	1.910	0.06248.
Significant levels: 0'***' 0.001'**' 0.01'*' 0.05'.' 0.1' '1 Multiple R-squared: 0.33 *p*-value: 0.0006				

3.4.2.2 Optimal UAV model

The performance of linear regression and exponential regression models derived from the UAV imagery were also assessed to obtain the optimal model. The best model was obtained with all combined features from the linear regression model (**Table 3.6).** In which after stepwise regression the model utilised for mapping included the spectral indices and the GLCM measures: GRVI, RGBVI, GCC, RCC, CL, GBVI, homogeneity dissimilarity. The model achieved the R^2 value of 0.28 and the *p*-value of 0.07 (**Table 3.8**).

© University of Venda

Table 3.8: The results obtained from the final linear model used for mapping palatable grass biomass derived from UAV image, with the validation metrics used to assess model accuracy.

UAV imagery				
Predictor	**Estimates**	**Std. Error**	***z* value**	***p* value**
(Intercept)	1094.174	347.919	3.145	0.00309**
GRVI	-1555.360	471.161	-3.301	0.00200 **
RGBVI	694.081	214.307	3.239	0.00238 **
GCC	-2082.709	786.998	-2.646	0.01149 *
RCC	-2085.096	631.199	-3.303	0.00199 **
CL	677.134	222.002	3.050	0.00400 **
GBVI	-60.380	18.726	-3.224	0.00248 **
Homogeneity	13.610	5.745	2.369	0.02263 *
Dissimilarity	3.610	1.828	1.747	0.08818 .
Significant levels: 0'***' 0.001'**' 0.01'*' 0.05'.' 0.1' '1 Multiple R-squared: 0.28 *p*-value: 0.07				

The optimal palatable grass biomass map produced from the PlanetScope subset image and the UAV image are depicted in **Figure 3.6** and **3.7** visually representing the biomass of the study. The results from the models have shown the PS subset image to outcompete the UAV data.

© University of Venda

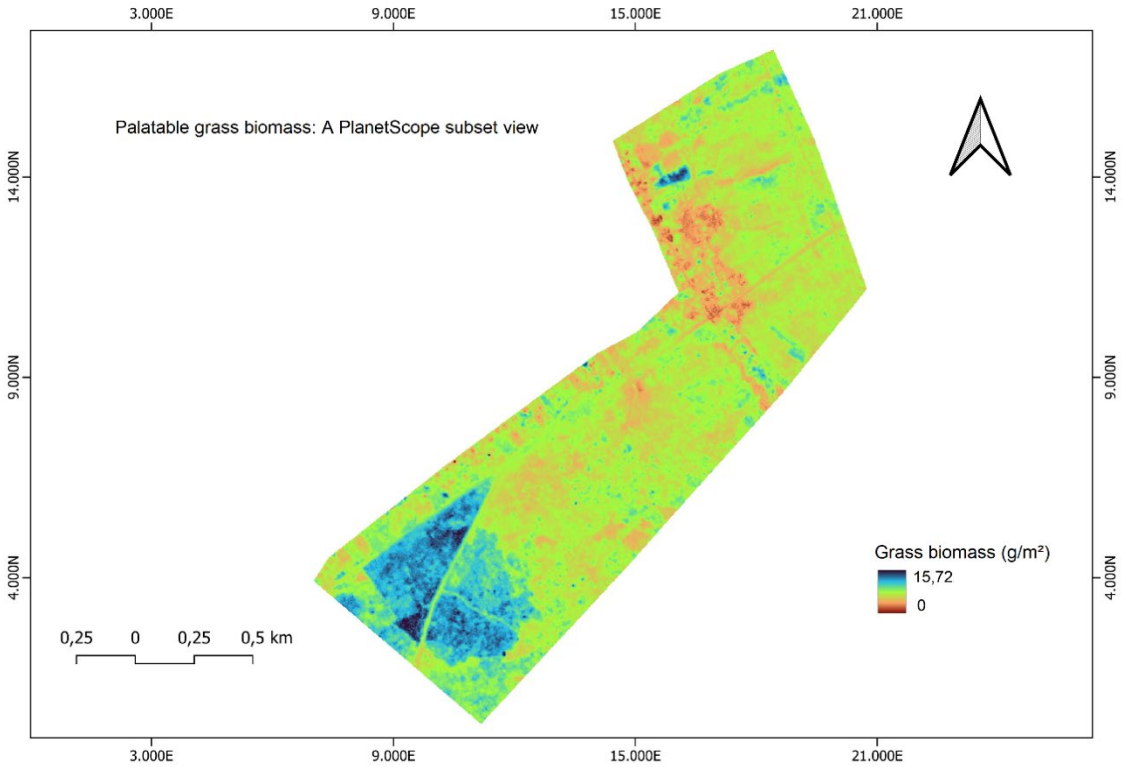
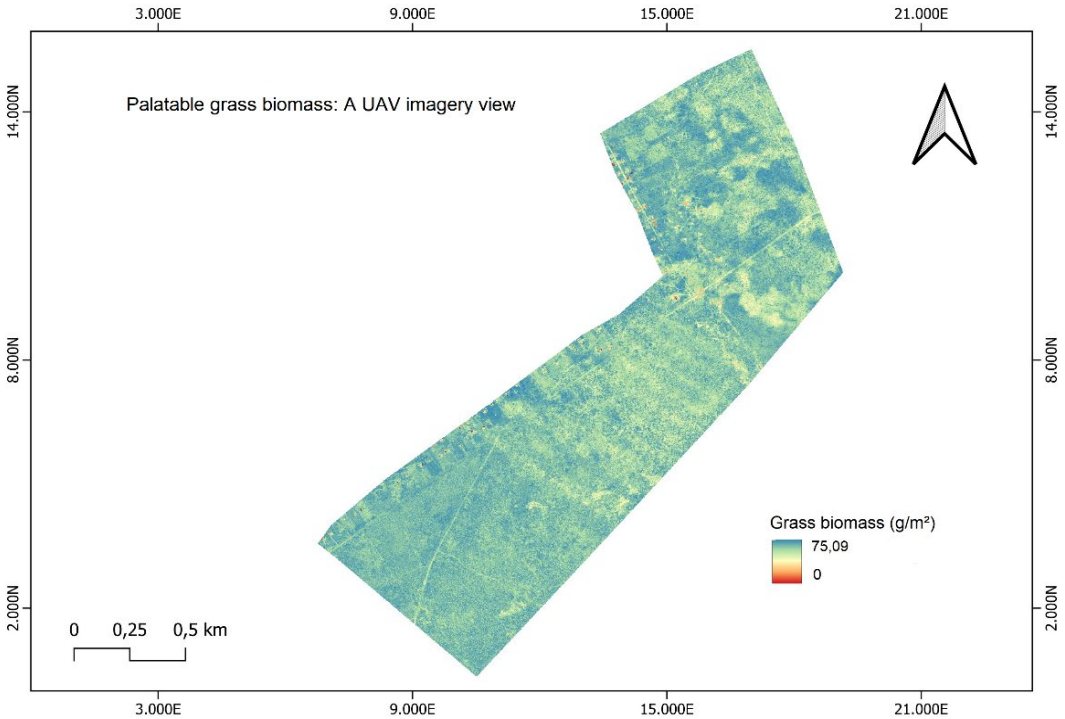


Figure 3.6: Palatable grass biomass spatial maps as predicted by the Linear model derived from the PlanetScope subset image.



© University of Venda

Figure 3.7: Palatable grass biomass spatial maps as predicted by the Linear model derived from the UAV imagery.

The observed versus the predicted palatable grass biomass for both the subset imagery and the UAV imagery showing their relationships are depicted in **Figure 3.8**. The R^2 value from the PlanetScope subset data (a) suggest that 34.63% of variation in the observed data was explained by the model and in contrast a weaker explanatory power was seen from the 22.05% of the UAV data (b).

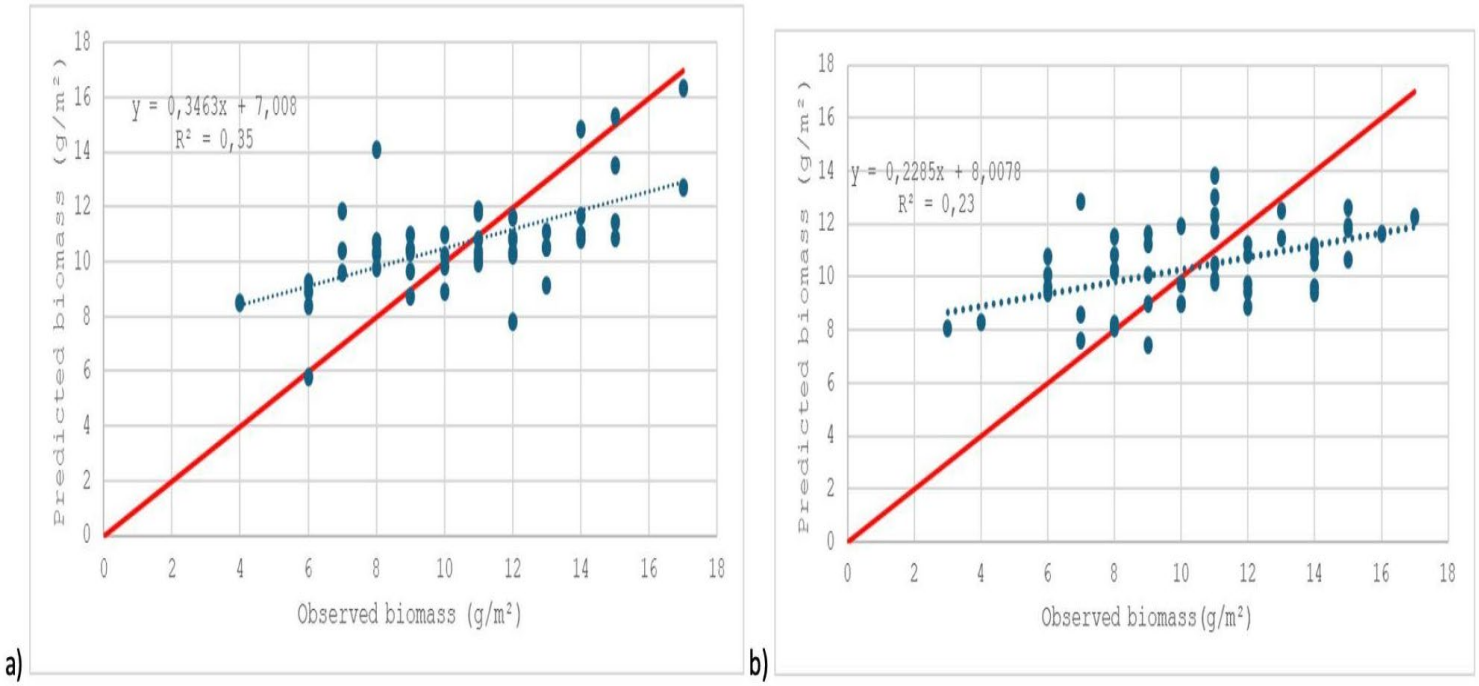


Figure 3.8: Scatterplots of the Measured vs. predicted palatable grass biomass, g/m²) by linear regression model from PlanetScope subset (a) and by a UAV imagery (b). A red line is provided as a reference line.

The statistical accuracy metrics of both the remote sensing data are visible in **Table 3.9**. The subset model obtained an RMSE of 2.36, MAE of 3.22 and R^2 of 0.35 while the UAV provided an RMSE of 6.57, MAE of 9.83 and R^2 of 0.23.

Table 3.9: Obtained validation metrics values from the PlanetScope subset image and UAV image.

© University of Venda

Validation			
Data source	**RMSE**	**MAE**	**R^2**
PlanetScope subset image	2.36	3.22	0.35
UAV imagery	9.83	6.57	0.23

RMSE = root mean squared Error, MAE = mean absolute error, R^2 = Coefficient of determination.

3.5 Discussion

The study's objectives were to (i) Compare the performance of linear and non-linear regression models for estimating palatable grass biomass using PlanetScope primary data and (ii) to compare the performance of linear and non-linear regression models for estimating palatable grass biomass using UAV data and PlanetScope subset data. Specifically, the purpose of the study was to compare the different models across the two data sources and determine the most robust modelling methods for mapping palatable grass biomass. Selection of optimal models requires intensive evaluation of different models (Awuah *et al*., 2020) and this is just what the study has done.

3.5.1 Palatable grass biomass estimation using PlanetScope primary imagery

The findings from the study demonstrated the power of the linear regression model with combined features (spectral bands, vegetation indices, and GLCM measures) as it outperformed the exponential models, as illustrated in the initial results obtained (**Table 3.6**). It is worth noting that, when used independently, certain individual predictor variables had initially shown poor to limited predictive power. However, significant predictive capabilities were established from the linear regression models. In particular, the linear regression model became robust with the addition of different predictor variables incorporated into the model. The model significantly improved with the integration of the spectral bands, vegetation indices, and the GLCM measures. Thus, this suggests that the combined features provide additional insights into the mapping of palatable grass biomass while highlighting the value of leveraging multiple variables for

© University of Venda

biomass mapping, moreover, enhancing palatable grass biomass estimation accuracy. In contrast, all exponential models exhibited the same pattern except for one case where the exponential model with combined variables outperformed all the other exponential models derived from that data source. The optimal model was with the combined features from the linear regression model. Nonetheless, despite advances in remote sensing, challenges remain. The combination of the three feature variables were unable to accurately predict and map the palatable grass biomass. After intensive model calibration, the use of a stepwise regression model provided a slightly robust model alternative. The model obtained from the stepwise regression leveraged a combination of three vegetation indices (NDVI, EVI, SAVI) and one GLCM measure (Variance) as the input parameters (**Table 3.7**).

In addition to the vegetation indices, the inclusion of the GLCM Variance offered valuable insights on the spatial texture characteristics while enhancing palatable grass biomass estimates accuracy by capturing the spectral and textural features (Dos Reis *et al*., 2020; Taddese *et al*., 2020). The model at hand obtained a relatively low R^2 value of 0.11 and an insignificant *p*-value of 0.25, indicating limited palatable grass biomass variance explained by the input variables and, furthermore, a non-reliable overall model. Contrary to any expectations, the model unexpectedly showed capabilities of palatable grass biomass mapping as compared to the previous models that seemed to have superior statistical significance but failed in map generation. Although the models' low R^2 value and insignificant *p*-value may suggest concerns against full reliance on the model for the prediction, its potential in generating a spatial representation of palatable grass biomass provides potential value in identifying specific patterns within the data.
Some studies have shown exponential models superior to linear regression models and often preferred over exponential models (Overman *et al*., 1994; Chapagain *et al*., 2014). However, most studies found that exponential models perform poorly in mapping biomass (Hamylton *et al*., 2020). Findings by (Hsieh, 2023) show that linear regression models perform better with outliers, however, exponential models often perform slightly better than the linear regression models. The biomass maps generated give valuable spatial insights for rangeland management and strategic grazing planning. Although the relatively low model accuracy may suggest insufficient precise biomass estimation by merely using remote sensing alone. The ability to identify areas with more or less palatable grass biomass helps small-scale farmers guide their livestock hence reducing overgrazing and improving rangeland sustainability. The model's predictive power

© University of Venda

could be enhanced with future studies by looking at possible conditions in which the model could thrive.

3.5.2 *Palatable grass biomass estimation using PlanetScope subset imagery and the UAV imagery*

The findings from the PlanetScope subset image align closely with the patterns derived from the primary image. The optimal model was obtained with the combined features from the linear regression model; however, it showed poor capabilities in palatable grass biomass map generation. The final model, including the NAVI, EVI, SAVI, and Variance, was derived from a stepwise regression process allowing for improved model's predictive power. The model obtained an R^2 value of 0.33 and a significant *p*-value of 0.0006 (**Table 3.7**), indicating vegetation indices and the GLCM measure being able to explain the palatable grass biomass variance by about 34.62%, suggesting a better fit to the model and that the relationships among the variables and the grass biomass are statistically significant. The performance metric's RMSE, MAE, and R^2 retrieved were 2.36, 3.22, and 0.33, respectively demonstrating the models ability to map spatial differences. The higher R^2 and significant *p*-value is indicative of improved predictive power as compared to the PlanetScope primary data. **Table 3.8** shows the results obtained from the optimal linear regression model computed with the UAV imagery, which includes six vegetation indices such as GRVI, RGBVI, GCC, RCC, CL, GBVI, and two GLCM measures, namely homogeneity and dissimilarity used for this model. This model resulted in each variable revealing statistical significance with the palatable grass biomass prediction. However, the overall R^2 value of 0.28 and a *p*-value of 0.07 suggest the model's regression coefficient is insignificant with selected variables while only explaining about 27.9% of the variance in biomass. **Figures 3.6** and **3.7** depict the palatable grass biomass spatial maps as predicted by the Linear model derived from the PlanetScope subset image and the UAV imagery. The biomass distribution as illustrated from the figures can be very beneficial to small-scale farmers by promoting sustainable grazing practices and consequently improve livestock production.

Based on the comparison between PlanetScope subset imagery and UAV imagery, it is clear that the optimal model for both data sources is achieved from the linear regression model with the combined features. The results from both the PlanetScope subset image and the UAV imagery (**Table 3.9**) is evident that the UAV imagery was inferior in predicting the palatable grass biomass as compared to the PlanetScope subset imagery. Though several studies have used the PlanetScope data and UAV data in mapping grass biomass, however, a few studies have compared their performances (Bazzo *et al*., 2023).

© University of Venda

The study by Bazzo et al. (2023) further explains that in the few studies that compared different sensors, palatable grass biomass accuracy was not significantly different from other sensors with the UAV RGB. Although inferiority performance may have been observed with the UAV as compared to other sensors (Nasi *et al*., 2018), their study also reveals the potential of the UAV mapping to producing good results to produce good results for reliable results to mapping grass biomass. The UAV's underperformance may be explained by: firstly, lack of multispectral capability and reliant on RGB sensors as compared to PlanetScope's multispectral properties may have limited its ability to accurately capture spectral features critical for biomass estimation (McCann *et al*., 2022). Secondly, the different data collection dates for PlanetScope (October) and UAV (December) may have introduced variability in vegetation conditions. With October being early wet season and December peak summer, UAV data likely captured matured dense grass as compared to the early growing stages captured by the PlanetScope imagery. Additionally, this might have been caused by the saturation effect as UAV's high spatial resolution may have introduced noise or overfitting due to sensors' saturation in dense canopies.

Overall, the study aligns with the results obtained by (Huete, 1988), who indicated the robustness of the linear regression technique, hence observing similar trends in the effective performance of these regression techniques. It is worth noting that with all three optimal models utilised for the PlanetScope primary image, the PlanetScope subset image, and the UAV imagery, the spectral bands were eliminated from the model in order to simplify and reduce possible data redundancy (Awuah *et al*., 2020) leaving the vegetation indices and the GLCM measures collectively accounting for a significant predictive potential. Spectral indices carry a strong correlation with vegetation biomass and moisture content (Awuah *et al*., 2020), and this could explain their high significance and role in these models. The inclusion of the GLCM features also reveals the importance of texture features captured by these features in the enhancement of these models for the palatable grass biomass prediction.

While the study provides valuable insights into palatable grass biomass distribution within the study area, it is important to consider the limitations presented. Firstly, the inability of the PlanetScope images to generate biomass maps may have impacted the study results. Secondly, palatable grass biomass estimation with remote sensing tools, especially with the use of UAV, poses challenges as rangelands have unique characteristics with diverse plant species that differ in developmental stages and size. Hence, to establish a robust model, future studies could consider factors such as the relationship with seasonal changes. Thirdly, the study acknowledges other limitations

© University of Venda

that may have emanated from the need for extensive data for model training and sensor limitations. Future studies should explore additional observation points as well as predictor variables that may provide new outcomes and insights through the improvement of the palatable grass biomass estimation models.

Although such limitations exist, the study offers useful information that can be used for successful rangeland management practices and decision-making by smallholder farmers and the community at large. The biomass maps generated show areas with high biomass areas and areas with low biomass; therefore, for instance, grazing activities could be considered in areas with high predicted palatable grass biomass values than areas with low predicted palatable grass biomass values. By doing so, more focus can be put on the low biomass areas for additional monitoring and management to promote growth and productivity for the grass species biomass in those areas. The commonly occurring palatable grass species within the study area are *Urochloa panicoides*, *Urochloa mosambicensis*, *Themeda triandra*, *Sporobolus africanus*, *Digitaria sanguinalis*, *Cynodon dactylon*, *Panicum maximum*. These are the areas where there is a high likelihood of cattle being able to feed and such plots with fewer plots cover show evidence of cattle or herbivores feeding on grass (dung, footprint in addition to evidence on the actual grass from being fed on).

3.6 Conclusion

This study investigated the performance of linear and non-linear regression models for estimating palatable grass biomass using remote sensing data from PlanetScope data and UAV data. Palatable grass biomass maps were created with the optimal models obtained from both the sensors utilised. Based on these findings, it is concluded that:

a) The study demonstrates the potential of both the linear and non-linear regression models for palatable grass biomass estimation. The former revealed its superior performance in all the models computed as it consistently outperformed non-linear (exponential) regression models across both sensors. The superior performance of the linear regression models emerged as clear patterns in response to both objectives.
b) The combination of spectral bands, indices, and GLCM measures in the models has shown improved performance compared to using them independently, thus helping us see the strength of each predictor variable. The elimination of the

© University of Venda

spectral bands and retention of both the spectral indices and GLCM features from all the optimal models exhibit a strong relationship with palatable grass biomass making them valuable predictors in the models. With the exception of the PlanetScope primary-based model with combined predictor variables, the non-linear regression models consistently showed weak predictive power. However, this suggests the competitiveness of the non-linear models against the linear models, proving that the input data (just as the combination of the variables) can influence the effectiveness of different modelling techniques.

c) The linear regression model derived from the PlanetScope subset image outperformed the linear regression model obtained from the UAV data; hence, the comparison between the PlanetScope subset image and UAV imagery has revealed its strength and ability to predict palatable grass biomass. This could be explained by the latter's wider spectral range which might have contributed to its ability to capture more detailed information on palatable grass biomass.

d) The study not only provides valuable insights for better understanding the strengths and limitations of the various models implemented in palatable grass biomass prediction and mapping but also offers information on the mapping of palatable grass biomass by using advanced remote sensing techniques and regression models to estimate the biomass. This contributes to land managers and policymakers making informed decisions on the sustainable use of rangelands and resource management.

© University of Venda

CHAPTER 4:

Conclusion and Synthesis

4.1 Introduction

The evaluation of grass biomass remains a crucial aspect of sustainable rangeland management, particularly in communal rangelands where excessive grazing is a critical concern. The study aimed to evaluate the biomass of palatable grass species in the communal rangeland using the integration of UAV data with high-resolution satellite data. The following specific objectives were accomplished to fulfil its primary objective: (1) to map the potential communal grazing areas in the Vhembe East villages, South Africa, and (2) to evaluate the performance of Linear and Non-linear regression models for mapping the quality of palatable grass biomass. In recent years, the knowledge of accurate information on the spatial distribution and condition of communal grazing areas has shown improvements with advancements in remote sensing techniques, such as satellite imagery and UAV imagery, offering promising opportunities. Knowledge of the distribution of palatable grass species in communal grazing areas is essential for livestock management. Mapping communal grazing areas using image classification is a technique that has been employed in numerous studies. The study also employed maximum likelihood as a classification model for mapping grazing areas. The study also employed the application of linear regression models and non-linear regression models for palatable grass biomass by using various predictor variables such as spectral bands, vegetation indices and GLCM measures retrieved from the remote sensing technologies.

4.2 To map the potential communal grazing areas in the Vhembe East villages, South Africa

With the use of PlanetScope data, the study assessed the potential of fine-scale PlanetScope data in mapping the potential grazing areas within the communal rangelands of the Vhembe East villages. The study employed maximum classification to accurately identify land cover classes within the study, such as water vegetation, built-up areas, grazing areas, and woodlands. The classification model reveals a robust correlation between the classified land cover types and the actual data. The model achieved high user and producer accuracies ranging from 93.31% to 100% which is indicative of an exceptional performance in identifying the different land cover classes within the study and more importantly the grazing areas with 100% for both the user's accuracy and producer's accuracies accounting for 50.30% of the total study area showing

© University of Venda

dominance. The study successfully extracted a detailed grazing area map that highlight the grazing areas' spatial distribution within the study. The classified map offers crucial insights into the area's landscape and insights into improved decision-making in the utilisation of the rangelands by both smallholder farmers and community members while consequently improving their livestock productivity.

4.3 To test the performance of linear and non-linear models for mapping palatable grass biomass using the unmanned aerial vehicle (UAV) and PlanetScope Data

The study's other objectives included performance comparison of linear and non-linear regression models for estimating palatable grass biomass using PlanetScope data and comparison performance of linear and non-linear regression models for estimating palatable grass biomass using UAV data and PlanetScope subset data. The study derived spectral bands, vegetation indices, and GLCM features from both the PlanetScope data and the UAV data, which were used as predictor variables in estimating palatable grass biomass. It was noted from the study that the integration of these variables showed improvements with the models computed as compared to single predictor variable use. The first model achieved an RMSE, MAE and R^2 of 2.16, 1.69 and 0.11, respectively, with a combination of three vegetation indices (NDVI, EVI, SAVI) and one GLCM measure (Variance) as the input parameters using the PlanetScope primary image. From the findings, the study concluded that the linear regression model outperformed the exponential model. Palatable grass biomass mapping for the PlanetScope data was achieved using this optimal model with the map showing the biomass distribution within the study area.

The use of the PlanetScope subset image also resulted in the model of three vegetation indices (NDVI, EVI, SAVI) and one GLCM measure (Variance) as the input parameters, aligning closely with the parameters utilised for the primary image. The RMSE, MAE and R^2 retrieved were 2.36, 3.22 and 0.35, respectively. The model from the UAV imagery included six vegetation indices such as GRVI, RGBVI, GCC, RCC, CL, GBVI, and two GLCM measures namely homogeneity and dissimilarity. The RMSE, MAE, and R2 of 9.8, 6.57, and 0.23 were obtained from the UAV imagery. The results from both the PlanetScope subset image and the UAV imagery is evident that the linear models performed better than the exponential models. Moreover, the linear regression model derived from the PlanetScope subset image outperformed the linear regression model obtained from the UAV data; hence, the comparison between the PlanetScope subset image and UAV imagery has revealed its strength and ability to predict palatable grass biomass.

4.4 Limitations and Recommendations

Several limitations do exist with both chapter 2 and chapter 3. PlanetScope has demonstrated its effectiveness in mapping grazing areas, however, opportunities do exist

© University of Venda

to improve the classification model for attaining a robust fine-scale resolution in estimating grazing areas. The study focused on the use of ML classification without exploring its comparison to other classification algorithms. The inclusion or comparison with other algorithms might have given a distinct perspective of the strength of the satellite image and the classification model. The study was conducted in poor communities which may not have easy access to the application of remote sensing technology as they require specialized skills and expertise. Such issues should be addressed by community-based monitoring systems implementations, enforced by the government, which could leverage local knowledge and resources and, hence, improve the overall condition of the grazing areas while promoting sustainable management practices. Future studies that address these issues will offer a better understanding of the potential grazing areas and their impact. The study also noted that the findings could have possibly been impacted the PlanetScope's inability to produce biomass map. One other limitation of the study emanated from the need for extensive data for model training. Future studies should explore additional observation points, predictor variables, and seasonal changes that may provide new outcomes and insights through the improvement of the Palatable grass biomass estimation models.

© University of Venda

REFERENCES

Abbas, Z., Jaber, H.S., 2020. Accuracy assessment of supervised classification methods for extraction land use maps using remote sensing and GIS techniques. IOP Conf. Ser. Mater. Sci. Eng. 745, 012166. https://doi.org/10.1088/1757-899X/745/1/012166

Abdullahi, A., Azah Samsudin, N., Rasidi Ibrahim, M., Syariff Aripin, M., Ahmad Khalid, S.K., Ali Othman, Z., 2020. Towards IR4.0 implementation in e-manufacturing: artificial intelligence application in steel plate fault detection. Indones. J. Electr. Eng. Comput. Sci. 20, 430. https://doi.org/10.11591/ijeecs.v20.i1.pp430-436

Acharki, S., 2022. PlanetScope contributions compared to Sentinel-2, and Landsat-8 for LULC mapping. Remote Sens. Appl. Soc. Environ. 27, 100774. https://doi.org/10.1016/j.rsase.2022.100774

Adam, E., Mutanga, O., Rugege, D., 2010. Multispectral and hyperspectral remote sensing for identification and mapping of wetland vegetation: a review. Wetl. Ecol. Manag. 18, 281–296. https://doi.org/10.1007/s11273-009-9169-z

Ali, I., Greifeneder, F., Stamenkovic, J., Neumann, M., Notarnicola, C., 2015. Review of Machine Learning Approaches for Biomass and Soil Moisture Retrievals from Remote Sensing Data. Remote Sens. 7, 16398–16421. https://doi.org/10.3390/rs71215841

Amadasun, M., King, R., 1989. Textural features corresponding to textural properties. IEEE Trans. Syst. Man Cybern. 19, 1264–1274. https://doi.org/10.1109/21.44046

Andreatta, D., Gianelle, D., Scotton, M., Dalponte, M., 2022.

Estimating grassland vegetation cover with remote sensing: A comparison between Landsat-8, Sentinel-2 and PlanetScope imagery. Ecol. Indic. 141, 109102. https://doi.org/10.1016/j.ecolind.2022.109102

Awuah, K.T., Aplin, P., Marston, C.G., Powell, I., Smit, I.P.J., 2020. Probabilistic Mapping and Spatial Pattern Analysis of Grazing Lawns in Southern African Savannahs Using WorldView-3 Imagery and Machine Learning Techniques. Remote Sens. 12, 3357. https://doi.org/10.3390/rs12203357

Bailey, D.W., 2004. Management strategies for optimal grazing distribution and use of arid rangelands. J. Anim. Sci. 82, E147-153.

Bazzo, C.O.G., Kamali, B., Hütt, C., Bareth, G., Gaiser, T., 2023. A Review of Estimation Methods for Aboveground Biomass in Grasslands Using UAV. Remote Sens. 15, 639. https://doi.org/10.3390/rs15030639

Bendig, J., Yu, K., Aasen, H., Bolten, A., Bennertz, S., Broscheit, J., Gnyp, M.L., Bareth, G., 2015. Combining UAV-based plant height from crop surface models, visible, and near infrared vegetation indices for biomass monitoring in barley. Int. J. Appl. Earth Obs. Geoinformation 39, 79–87. https://doi.org/10.1016/j.jag.2015.02.012

© University of Venda

Bennett, J., Barrett, H., 2007. Rangeland as a Common Property Resource: Contrasting Insights from Communal Areas of Central Eastern Cape Province, South Africa. Hum. Ecol. 35, 97–112. https://doi.org/10.1007/s10745-006-9062-9

Bharatkar, P., Patel, R., 2013. Approach to accuracy assessment for RS image classification techniques. Int. J. Sci. Eng. Res. 4, 79–86.

Bolo, P., Sommer, R., Kihara, J., M., K., Nyawira, S., Notenbaert, A., 2019. RANGELAND DEGRADATION - CAUSES CONSEQUENCES MONITORING TECHNIQUES AND REMEDIES (1).

Boval, M., Dixon, R.M., 2012. The importance of grasslands for animal production and other functions: a review on management and methodological progress in the tropics. animal 6, 748–762. https://doi.org/10.1017/S1751731112000304

Chaminuka, P., Udo, H.M.J., Eilers, K.C.H.A.M., Van Der Zijpp, A., 2014. Livelihood roles of cattle and prospects for alternative land uses at the wildlife/livestock interface in South Africa. Land Use Policy 38, 80–90. https://doi.org/10.1016/j.landusepol.2013.10.007

Chapagain, T.R., Sharma, R.P., Bhandari, S.K., 2014. Modeling above-ground biomass for three tropical tree species at their juvenile stage. For. Sci. Technol. 10, 51–60. https://doi.org/10.1080/21580103.2013.834277

Chen, R.-C., Dewi, C., Huang, S.-W., Caraka, R.E., 2020. Selecting critical features for data classification based on machine learning methods. J. Big Data 7, 52. https://doi.org/10.1186/s40537-020-00327-4

Cheng, Y., Vrieling, A., Fava, F., Meroni, M., Marshall, M., Gachoki, S., 2020. Phenology of short vegetation cycles in a Kenyan rangeland from PlanetScope and Sentinel-2. Remote Sens. Environ. 248, 112004. https://doi.org/10.1016/j.rse.2020.112004

Chicco, D., Warrens, M.J., Jurman, G., 2021. The coefficient of determination R-squared is more informative than SMAPE, MAE, MAPE, MSE and RMSE in regression analysis evaluation. PeerJ Comput. Sci. 7, e623.

Clementini, C., Pomente, A., Latini, D., Kanamaru, H., Vuolo, M.R., Heureux, A., Fujisawa, M., Schiavon, G., Del Frate, F., 2020. Long-Term Grass Biomass Estimation of Pastures from Satellite Data. Remote Sens. 12, 2160. https://doi.org/10.3390/rs12132160

Corti, M., Cavalli, D., Cabassi, G., Bechini, L., Pricca, N., Paolo, D., Marinoni, L., Vigoni, A., Degano, L., Marino Gallina, P., 2023. Improved estimation of herbaceous crop aboveground biomass using UAV-derived crop height combined with vegetation indices. Precis. Agric. 24, 587–606. https://doi.org/10.1007/s11119-022-09960-w

Department of Agriculture, Forestry and Fisheries (DAFF), 2013. Annual Report 2013/14. Department of Agriculture, Forestry and Fisheries (DAFF), South Africa: DAFF.

Dobrinić, D., Gašparović, M., Medak, D., 2022. EVALUATION OF FEATURE SELECTION METHODS FOR VEGETATION MAPPING USING MULTITEMPORAL SENTINEL IMAGERY. Int. Arch. Photogramm. Remote Sens.

© University of Venda

Spat. Inf. Sci. XLIII-B3-2022, 485–491. https://doi.org/10.5194/isprs-archives-XLIII-B3-2022-485-2022

Dos Reis, A.A., Werner, J.P.S., Silva, B.C., Figueiredo, G.K.D.A., Antunes, J.F.G., Esquerdo, J.C.D.M., Coutinho, A.C., Lamparelli, R.A.C., Rocha, J.V., Magalhães, P.S.G., 2020. Monitoring Pasture Aboveground Biomass and Canopy Height in an Integrated Crop–Livestock System Using Textural Information from PlanetScope Imagery. Remote Sens. 12, 2534. https://doi.org/10.3390/rs12162534

Eng, L., Ismail, R., Hashim, W., Baharum, A., 2019. The Use of VARI, GLI, and VIgreen Formulas in Detecting Vegetation In aerial Images. Int. J. Technol. 10, 1385. https://doi.org/10.14716/ijtech.v10i7.3275

Erunova, M.G., Pisman, T.I., Shevyrnogov, A.P., Ерунова, М.Г., Письман, Т.И., Шевырногов, А.П., 2021. The Technology for Detecting Weeds in Agricultural Crops Based on Vegetation Index VARI (PlanetScope). PlanetScope. https://doi.org/10.17516/1999-494X-0314

European Space Agency, 2022. Sentinel Application Tool (SNAP).

Falkowski, M.J., Gessler, P.E., Morgan, P., Hudak, A.T., Smith, A.M.S., 2005. Characterizing and mapping forest fire fuels using ASTER imagery and gradient modeling. For. Ecol. Manag. 217, 129–146. https://doi.org/10.1016/j.foreco.2005.06.013

Fenetahun, Y., Yuan, Y., Xinwen, X., Fentahun, T., Nzabarinda, V., Yong-dong, W., 2021. Impact of Grazing Intensity on Soil Properties in Teltele Rangeland, Ethiopia. Front. Environ. Sci. 9, 664104. https://doi.org/10.3389/fenvs.2021.664104

Frazier, A.E., Hemingway, B.L., 2021. A Technical Review of Planet Smallsat Data: Practical Considerations for Processing and Using PlanetScope Imagery. Remote Sens. 13, 3930. https://doi.org/10.3390/rs13193930

Gallant, E., LaRocque, A., Leblon, B., Douglas, A., 2021. EELGRASS MAPPING WITH SENTINEL-2 AND UAV DATA IN PRINCE EDWARD ISLAND (CANADA). ISPRS Ann. Photogramm. Remote Sens. Spat. Inf. Sci. V-3–2021, 125–132. https://doi.org/10.5194/isprs-annals-V-3-2021-125-2021

Getabalew, M., Alemneh, T., 2019. Factors affecting the productivity of rangelands. MedPub J. 3, 19.

Gitelson, A.A., Kaufman, Y.J., Merzlyak, M.N., 1996. Use of a green channel in remote sensing of global vegetation from EOS-MODIS. Remote Sens. Environ. 58, 289–298. https://doi.org/10.1016/S0034-4257(96)00072-7

Gitelson, A.A., Kaufman, Y.J., Stark, R., Rundquist, D., 2002. Novel algorithms for remote estimation of vegetation fraction. Remote Sens. Environ. 80, 76–87. https://doi.org/10.1016/S0034-4257(01)00289-9

Godde, C.M., Boone, R.B., Ash, A.J., Waha, K., Sloat, L.L., Thornton, P.K., Herrero, M., 2020. Global rangeland production systems and livelihoods at threat under climate change and variability. Environ. Res. Lett. 15, 044021. https://doi.org/10.1088/1748-9326/ab7395

© University of Venda

Gorade, P.D., Datar, M.N., 2014. Checklist of Palatable Grass Species from Peninsular India. Not. Sci. Biol. 6, 441–447. https://doi.org/10.15835/nsb649376

Gruner, E., Wachendorf, M., Astor, T., 2020. The potential of UAV-borne spectral and textural information for predicting aboveground biomass and N fixation in legume-grass mixtures. PLOS ONE 15, e0234703. https://doi.org/10.1371/journal.pone.0234703

Gusha, B., Palmer, A.R., Zondani, T.C., 2023. Assessing Livestock Grazing Distribution in Communal Rangelands of the Eastern Cape, South Africa: Towards Monitoring Livestock Movements in Rangelands. Land 12, 760. https://doi.org/10.3390/land12040760

Hall-Beyer, M., 2017. GLCM Texture: A Tutorial v. 3.0 March 2017.

Hamylton, S.M., Morris, R.H., Carvalho, R.C., Roder, N., Barlow, P., Mills, K., Wang, L., 2020. Evaluating techniques for mapping island vegetation from unmanned aerial vehicle (UAV) images: Pixel classification, visual interpretation and machine learning approaches. Int. J. Appl. Earth Obs. Geoinformation 89, 102085. https://doi.org/10.1016/j.jag.2020.102085

Haralick, R.M., Shanmugam, K., Dinstein, I., 1973. Textural Features for Image Classification. IEEE Trans. Syst. Man Cybern. SMC-3, 610–621. https://doi.org/10.1109/TSMC.1973.4309314

Hilbert, D., 2001. The utility of artificial neural networks for modelling the distribution of vegetation in past, present and future climates. Ecol. Model. 146, 311–327. https://doi.org/10.1016/S0304-3800(01)00323-4

Hsieh, W.W., 2023. Improving Predictions by Nonlinear Regression Models from Outlying Input Data. J. Environ. Inform. 41, 75–87.

Huete, A.R., 1988. A soil-adjusted vegetation index (SAVI). Remote Sens. Environ. 25, 295–309. https://doi.org/10.1016/0034-4257(88)90106-X

Hunt, E.R., Everitt, J.H., Ritchie, J.C., Moran, M.S., Booth, D.T., Anderson, G.L., Clark, P.E., Seyfried, M.S., 2003. Applications and Research Using Remote Sensing for Rangeland Management. Photogramm. Eng. Remote Sens. 69, 675–693. https://doi.org/10.14358/PERS.69.6.675

Iqbal, N., Mumtaz, R., Shafi, U., Zaidi, S.M.H., 2021. Gray level co-occurrence matrix (GLCM) texture based crop classification using low altitude remote sensing platforms. PeerJ Comput. Sci. 7, e536. https://doi.org/10.7717/peerj-cs.536

Issa, S., Dahy, B., Ksiksi, T., Saleous, N., 2020. A Review of Terrestrial Carbon Assessment Methods Using Geo-Spatial Technologies with Emphasis on Arid Lands. Remote Sens. 12, 2008. https://doi.org/10.3390/rs12122008

Jamsranjav, C., Fernández-Giménez, M.E., Reid, R.S., Adya, B., 2019. Opportunities to integrate herders' indicators into formal rangeland monitoring: an example from Mongolia. Ecol. Appl. 29, e01899. https://doi.org/10.1002/eap.1899

© University of Venda

Jovanovic, N., Garcia, C., Bugan, R., Teich, I., Rodriguez, C., 2014. Validation of remotely-sensed evapotranspiration and NDWI using ground measurements at Riverlands, South Africa. Water SA 40, 211. https://doi.org/10.4314/wsa.v40i2.3

Kakembo, V., Ndou, N., 2019. Relating vegetation condition to grazing management systems in the central Keiskamma Catchment, Eastern Cape Province, South Africa. Land Degrad. Dev. 30, 1052–1060. https://doi.org/10.1002/ldr.3292

Kamwi, J.M., Kaetsch, C., Graz, F.P., Chirwa, P., Manda, S., 2017. Trends in land use and land cover change in the protected and communal areas of the Zambezi Region, Namibia. Environ. Monit. Assess. 189, 242. https://doi.org/10.1007/s10661-017-5934-2

Kaul, H.A., Ingle, S., 2012. Land Use Land Cover Classification and Change Detection Using High Resolution Temporal Satellite Data. J. Environ. 1, 146–152.

Kellner, K., Moussa, A.S., 2009. A conceptual tool for improving rangeland management decision-making at grassroots level: the local-level monitoring approach. Afr. J. Range Forage Sci. 26, 139–147. https://doi.org/10.2989/AJRF.2009.26.3.5.950

Kelsey, K.C., Neff, J.C., 2014. Estimates of Aboveground Biomass from Texture Analysis of Landsat Imagery. Remote Sens. 6, 6407–6422. https://doi.org/10.3390/rs6076407

Koko, A.F., Wu, Y., Abubakar, G.A., Alabsi, A.A.N., Hamed, R., Bello, M., 2021. Thirty Years of Land Use/Land Cover Changes and Their Impact on Urban Climate: A Study of Kano Metropolis, Nigeria. Land 10, 1106. https://doi.org/10.3390/land10111106

Lefulebe, B.E., Van Der Walt, A., Xulu, S., 2022. Fine-Scale Classification of Urban Land Use and Land Cover with PlanetScope Imagery and Machine Learning Strategies in the City of Cape Town, South Africa. Sustainability 14, 9139. https://doi.org/10.3390/su14159139

Letsoalo, N.L., 2019. Rangeland management practices among emerging livestock farmers in Gauteng province, South Africa.

Li, C., Zhou, L., Xu, W., 2021. Estimating Aboveground Biomass Using Sentinel-2 MSI Data and Ensemble Algorithms for Grassland in the Shengjin Lake Wetland, China. Remote Sens. 13, 1595. https://doi.org/10.3390/rs13081595

Liu, H., Dahlgren, R., Larsen, R., Devine, S., Roche, L., O' Geen, A., Wong, A., Covello, S., Jin, Y., 2019. Estimating Rangeland Forage Production Using Remote Sensing Data from a Small Unmanned Aerial System (sUAS) and PlanetScope Satellite. Remote Sens. 11, 595. https://doi.org/10.3390/rs11050595

Maimaitijiang, M., Sagan, V., Sidike, P., Daloye, A.M., Erkbol, H., Fritschi, F.B., 2020. Crop Monitoring Using Satellite/UAV Data Fusion and Machine Learning. Remote Sens. 12, 1357. https://doi.org/10.3390/rs12091357

Malahlela, O., Cho, M.A., Mutanga, O., 2014. Mapping canopy gaps in an indigenous subtropical coastal forest using high-resolution WorldView-2 data. Int. J. Remote Sens. 35, 6397–6417. https://doi.org/10.1080/01431161.2014.954061

© University of Venda

Mangani, T., Marquart, A., Chirima, G., Kellner, K., 2022. Grass species diversity response to brush packing in semi-arid rangelands of South Africa. J. Arid Environ. 207, 104832. https://doi.org/10.1016/j.jaridenv.2022.104832

Marques, M.J., Alvarez, A., Carral, P., Sastre, B., Bienes, R., 2020. The use of remote sensing to detect the consequences of erosion in gypsiferous soils. Int. Soil Water Conserv. Res., Soil erosion assessment tools and data; creation, consolidation, and harmonization – A special issue from the Global Symposium on Soil Erosion 2019 (Rome, FAO HQ). 8, 383–392. https://doi.org/10.1016/j.iswcr.2020.10.001

Masiteng, J.T., Van der Westhuizen, C., Mantli, M., 2003. Aspirations and needs of farmers on communal grazing areas in the Free State. South Afr. J. Agric. Ext. 32, 85–97. https://doi.org/10.4314/SAJAE.V32I1.3652

Mbatha, C., 2021. Livestock production and marketing for small emerging farmers in South Africa and Kenya: comparative lessons. South Afr. J. Agric. Ext. SAJAE 49, 141–161. https://doi.org/10.17159/2413-3221/2021/v49n1a10783

McCann, J.A., Keith, D.A., Kingsford, R.T., 2022. Measuring plant biomass remotely using drones in arid landscapes. Ecol. Evol. 12, e8891. https://doi.org/10.1002/ece3.8891

McGranahan, D.A., Kirkman, K.P., 2013. Multifunctional Rangeland in Southern Africa: Managing for Production, Conservation, and Resilience with Fire and Grazing. Land 2, 176–193. https://doi.org/10.3390/land2020176

Mdiya, L., Taruvinga, A., Mushunje, A., Mopipi, K., Ngarava, S., 2021. Rural community use and perception of rangeland products in Eastern Cape Province, South Africa. Afr. J. Sci. Technol. Innov. Dev. 13, 757–768. https://doi.org/10.1080/20421338.2020.1798043

Mekuria, W., 2013. Conversion of Communal Grazing Lands into Exclosures Restored Soil Properties in the Semi-Arid Lowlands of Northern Ethiopia. Arid Land Res. Manag. 27, 153–166. https://doi.org/10.1080/15324982.2012.721858

Mohammadpour, P., Viegas, D.X., Viegas, C., 2022. Vegetation Mapping with Random Forest Using Sentinel 2 and GLCM Texture Feature—A Case Study for Lousã Region, Portugal. Remote Sens. 14, 4585. https://doi.org/10.3390/rs14184585

Mudau, H.S., Msiza, N.H., Sipango, N., Ravhuhali, K.E., Mokoboki, H.K., Moyo, B., 2022. Veld restoration strategies in South African semi-arid rangelands. Are there any successes?—A review. Front. Environ. Sci. 10, 960345. https://doi.org/10.3389/fenvs.2022.960345

Murei, A., Mogane, B., Mothiba, D.P., Mochware, O.T.W., Sekgobela, J.M., Mudau, M., Musumuvhi, N., Khabo-Mmekoa, C.M., Moropeng, R.C., Momba, M.N.B., 2022. Barriers to Water and Sanitation Safety Plans in Rural Areas of South Africa—A Case Study in the Vhembe District, Limpopo Province. Water 14, 1244. https://doi.org/10.3390/w14081244

Mutanga, O., Skidmore, A.K., 2004. Narrow band vegetation indices overcome the saturation problem in biomass estimation. Int. J. Remote Sens. 25, 3999–4014. https://doi.org/10.1080/01431160310001654923

© University of Venda

Naicker, R., Mutanga, O., Peerbhay, K., Odebiri, O., 2024. Estimating high-density aboveground biomass within a complex tropical grassland using Worldview-3 imagery. Environ. Monit. Assess. 196, 370. https://doi.org/10.1007/s10661-024-12476-7

Nakano, T., Bat-Oyun, T., Shinoda, M., 2020. Responses of palatable plants to climate and grazing in semi-arid grasslands of Mongolia. Glob. Ecol. Conserv. 24, e01231. https://doi.org/10.1016/j.gecco.2020.e01231

Nasi, R., Viljanen, N., Kaivosoja, J., Alhonoja, K., Hakala, T., Markelin, L., Honkavaara, E., 2018. Estimating Biomass and Nitrogen Amount of Barley and Grass Using UAV and Aircraft Based Spectral and Photogrammetric 3D Features. Remote Sens. 10, 1082. https://doi.org/10.3390/rs10071082

Nawaz, A., Iqbal, Z., Ullah, S., 2015. Performance analysis of supervised image classification techniques for the classification of multispectral satellite imagery, in: 2015 Fourth International Conference on Aerospace Science and Engineering (ICASE). Presented at the 2015 Fourth International Conference on Aerospace Science and Engineering (ICASE), IEEE, Islamabad, Pakistan, pp. 1–5. https://doi.org/10.1109/ICASE.2015.7489513

Nguyen, T.D., Kappas, M., 2020. Estimating the Aboveground Biomass of an Evergreen Broadleaf Forest in Xuan Lien Nature Reserve, Thanh Hoa, Vietnam, Using SPOT-6 Data and the Random Forest Algorithm. Int. J. For. Res. 2020, e4216160. https://doi.org/10.1155/2020/4216160

Norovsuren, B., Tseveen, B., Batomunkuev, V., Renchin, T., Natsagdorj, E., Yangiv, A., Mart, Z., 2019. Land cover classification using maximum likelihood method (2000 and 2019) at Khandgait valley in Mongolia. IOP Conf. Ser. Earth Environ. Sci. 381, 012054. https://doi.org/10.1088/1755-1315/381/1/012054

O'Connell, J.L., Alber, M., 2016. A smart classifier for extracting environmental data from digital image time-series: Applications for PhenoCam data in a tidal salt marsh. Environ. Model. Softw. 84, 134–139. https://doi.org/10.1016/j.envsoft.2016.06.025

Overman, J.P.M., Witte, H.J.L., Saldarriaga, J.G., 1994. Evaluation of regression models for above-ground biomass determination in Amazon rainforest. J. Trop. Ecol. 10, 207–218. https://doi.org/10.1017/S0266467400007859

Owusu-Adjei, M., Hayfron-Acquah, J.B., Frimpong, T., Abdul-Salaam, G., 2023. A systematic review of prediction accuracy as an evaluation measure for determining machine learning model performance in healthcare systems. https://doi.org/10.1101/2023.06.01.23290837

Palamuleni, L., Annegarn, H., Kneen, M., Landmann, T., 2007. Mapping rural savanna woodlands in malawi: a comparison of maximum likelihood and fuzzy classifiers., in: 2007 IEEE International Geoscience and Remote Sensing Symposium. Presented at the 2007 IEEE International Geoscience and Remote Sensing Symposium, IEEE, Barcelona, Spain, pp. 1260–1264. https://doi.org/10.1109/IGARSS.2007.4423035

© University of Venda

Parente, L., Taquary, E., Silva, A., Souza, C., Ferreira, L., 2019. Next Generation Mapping: Combining Deep Learning, Cloud Computing, and Big Remote Sensing Data. Remote Sens. 11, 2881. https://doi.org/10.3390/rs11232881

Patil, M.S., Kambekar, A.R., 2022. Floodplain Mapping Using Hydraulic Simulation and Geographic Information System. Indian J. Sci. Technol. 15, 2027–2036. https://doi.org/10.17485/IJST/v15i39.1056

Pfeiffer, M., Hoffmann, M.P., Scheiter, S., Nelson, W., Isselstein, J., Ayisi, K., Odhiambo, J.J., Rötter, R., 2022. Modeling the effects of alternative crop–livestock management scenarios on important ecosystem services for smallholder farming from a landscape perspective. Biogeosciences 19, 3935–3958. https://doi.org/10.5194/bg-19-3935-2022

Planet Labs Inc, 2023. Planet Imagery and Archive. [WWW Document]. URL https://www.planet.com/products/planet-imagery (accessed 1.5.23).

QGIS Development Team, 2022. QGIS Geographic Information System. Open Source Geospatial Foundation Project.

Quang, N.H., Quinn, C.H., Carrie, R., Stringer, L.C., Hue, L.T.V., Hackney, C.R., Tan, D.V., 2022. Comparisons of regression and machine learning methods for estimating mangrove above-ground biomass using multiple remote sensing data in the red River Estuaries of Vietnam. Remote Sens. Appl. Soc. Environ. 26, 100725. https://doi.org/10.1016/j.rsase.2022.100725

R Core Team, 2022. R: A language and environment for statistical computing. R Foundation for Statistical Computing, Vienna, Austria.

Ramoelo, A., Cho, M., Mathieu, R., Skidmore, A.K., 2015. Potential of Sentinel-2 spectral configuration to assess rangeland quality. J. Appl. Remote Sens. 9, 094096. https://doi.org/10.1117/1.JRS.9.094096

Rapiya, M., Ramoelo, A., Truter, W., 2023. Seasonal evaluation and mapping of aboveground biomass in natural rangelands using Sentinel-1 and Sentinel-2 data. Environ. Monit. Assess. 195, 1544. https://doi.org/10.1007/s10661-023-12133-5

Rhodes, E.C., Perotto-Baldivieso, H.L., Reeves, M.C., Gonzalez, L.A., 2022. Perspectives on the Special Issue for Applications of Remote Sensing for Livestock and Grazingland Management. Remote Sens. 14, 1882. https://doi.org/10.3390/rs14081882

Romero, M., Luo, Y., Su, B., Fuentes, S., 2018. Vineyard water status estimation using multispectral imagery from an UAV platform and machine learning algorithms for irrigation scheduling management. Comput. Electron. Agric. 147, 109–117. https://doi.org/10.1016/j.compag.2018.02.013

Rouse, J.W., Haas, R.H., Schell, J.A., Deering, D.W., 1974. Monitoring vegetation systems in the Great Plains with ERTS.

Sandhage-Hofmann, A., Kotzé, E., van Delden, L., Dominiak, M., Fouché, H.J., van der Westhuizen, H.C., Oomen, R.J., du Preez, C.C., Amelung, W., 2015. Rangeland management effects on soil properties in the savanna biome, South Africa: A case

© University of Venda

study along grazing gradients in communal and commercial farms. J. Arid Environ. 120, 14–25. https://doi.org/10.1016/j.jaridenv.2015.04.004

Schill, S.R., McNulty, V.P., Pollock, F.J., Lüthje, F., Li, J., Knapp, D.E., Kington, J.D., McDonald, T., Raber, G.T., Escovar-Fadul, X., Asner, G.P., 2021. Regional High-Resolution Benthic Habitat Data from Planet Dove Imagery for Conservation Decision-Making and Marine Planning. Remote Sens. 13, 4215. https://doi.org/10.3390/rs13214215

Sebola, M.P., Mamabolo, M.A.M., University of Limpopo, South Africa, 2020. Governing and managing communal land as a resource in South Africa: A case of selected communal property associations in Vhembe district, Limpopo province. Bus. Manag. Rev. 11. https://doi.org/10.24052/BMR/V11NU01/ART-01

Serbin, G., Daughtry, C.S.T., Hunt, E.R., Reeves, J.B., Brown, D.J., 2009. Effects of soil composition and mineralogy on remote sensing of crop residue cover. Remote Sens. Environ. 113, 224–238. https://doi.org/10.1016/j.rse.2008.09.004

Sharifi, A., Felegari, S., 2023. Remotely sensed normalized difference red-edge index for rangeland biomass estimation. Aircr. Eng. Aerosp. Technol. 95, 1128–1136. https://doi.org/10.1108/AEAT-07-2022-0199

Sibanda, M., Mutanga, O., Rouget, M., Kumar, L., 2017. Estimating Biomass of Native Grass Grown under Complex Management Treatments Using WorldView-3 Spectral Derivatives. Remote Sens. 9, 55. https://doi.org/10.3390/rs9010055

Sibanda, M., Onisimo, M., Dube, T., Mabhaudhi, T., 2021. Quantitative assessment of grassland foliar moisture parameters as an inference on rangeland condition in the mesic rangelands of southern Africa. Int. J. Remote Sens. 42, 1474–1491. https://doi.org/10.1080/01431161.2020.1832282

Sikhweni, Hassan, 2014. Opportunities and challenges facing small-scale cattle farmers living adjacent to Kruger National Park, Limpopo Province. J. Emerg. Trends Econ. Manag. Sci. 5, 38–43.

Sikhweni, Hassan, 2014a. Determinants of herd size among small-scale cattle farmers: the case of selected villages at the Mhinga Traditional Authority in Limpopo, South Africa. Agrekon 53, 106–122. https://doi.org/10.1080/03031853.2014.974945

Singh, L., Mutanga, O., Mafongoya, P., Peerbhay, K.Y., 2018. Multispectral mapping of key grassland nutrients in KwaZulu-Natal, South Africa. J. Spat. Sci. 63, 155–172.

Sinthumule, N.I., Mzamani, L.C.M., 2019. Communities and Conservation: Marula Trees (*Sclerocarya birrea* subsp. *caffra*) Under Communal Management at Matiyane Village, Limpopo Province, South Africa. Trop. Conserv. Sci. 12, 194008291982896. https://doi.org/10.1177/1940082919828969

Sisodia, P.S., Tiwari, V., Kumar, A., 2014. Analysis of Supervised Maximum Likelihood Classification for remote sensing image, in: International Conference on Recent Advances and Innovations in Engineering (ICRAIE-2014). Presented at the 2014 Recent Advances and Innovations in Engineering (ICRAIE), IEEE, Jaipur, India, pp. 1–4. https://doi.org/10.1109/ICRAIE.2014.6909319

© University of Venda

Steinfeld, H., Gerber, P., Wassenaar, T., Castel, V., Rosales, M., De Haan, C., 2006. Livestock's Long Shadow-Environmental Issues and Options. Food and Agriculture (FAO) of the United Nations document. Rome: FAO Publishing Management Service.

Svinurai, W., 2020. Use of remote sensing in native grass biomass modelling to estimate range productivity and animal performance in a tree-shrub savanna in southern Zimbabwe (Thesis). University of Pretoria.

Svinurai, W., Hassen, A., Tesfamariam, E., Ramoelo, A., Cullen, B., 2021. Calibration and evaluation of the Sustainable Grazing Systems pasture model for predicting native grass aboveground biomass production in southern Africa. Afr. J. Range Forage Sci. 38, S28–S40. https://doi.org/10.2989/10220119.2021.1875501

Svoray, T., Perevolotsky, A., Atkinson, P.M., 2013. Ecological sustainability in rangelands: the contribution of remote sensing. Int. J. Remote Sens. 34, 6216–6242. https://doi.org/10.1080/01431161.2013.793867

Taddese, H., Asrat, Z., Burud, I., Gobakken, T., Ørka, H.O., Dick, Ø.B., Næsset, E., 2020. Use of Remotely Sensed Data to Enhance Estimation of Aboveground Biomass for the Dry Afromontane Forest in South-Central Ethiopia. Remote Sens. 12, 3335. https://doi.org/10.3390/rs12203335

Tapamo, H., Mfopou, A., Ngonmang, B., Couteron, P., Monga, O., 2014. Linear vs non-linear learning methods A comparative study for forest above ground biomass, estimation from texture analysis of satellite images. Rev. Afr. Rech. En Inform. Mathématiques Appliquées Volume 18, 2014, 1982. https://doi.org/10.46298/arima.1982

Tatachar, A.V., 2021. Comparative assessment of regression models based on model evaluation metrics. Int. Res. J. Eng. Technol. IRJET 8, 2395–0056.

Tavirimirwa, B., Manzungu, E., Washaya, S., Ncube, Sharai, Ncube, Shadreck, Mudzengi, C., Mwembe, R., 2019. Efforts to improve Zimbabwe communal grazing areas: a review. Afr. J. Range Forage Sci. 36, 73–83.

Théau, J., Lauzier-Hudon, É., Aube, L., Devillers, N., 2021. Estimation of forage biomass and vegetation cover in grasslands using UAV imagery. PloS One 16, e0245784.

Traore, A., Mawenda, J., Komba, A., 2018. Land-Cover Change Analysis and Simulation in Conakry (Guinea), Using Hybrid Cellular-Automata and Markov Model. Urban Sci. 2, 39. https://doi.org/10.3390/urbansci2020039

Tsegaye, D., Moe, S.R., Vedeld, P., Aynekulu, E., 2010. Land-use/cover dynamics in Northern Afar rangelands, Ethiopia. Agric. Ecosyst. Environ. 139, 174–180. https://doi.org/10.1016/j.agee.2010.07.017

Tucker, C.J., 1979. Red and photographic infrared linear combinations for monitoring vegetation. Remote Sens. Environ. 8, 127–150. https://doi.org/10.1016/0034-4257(79)90013-0

© University of Venda

Vetter, S., 2013. Development and sustainable management of rangeland commons – aligning policy with the realities of South Africa's rural landscape. Afr. J. Range Forage Sci. 30, 1–9. https://doi.org/10.2989/10220119.2012.750628

Viljanen, N., Honkavaara, E., Näsi, R., Hakala, T., Niemeläinen, O., Kaivosoja, J., 2018. A Novel Machine Learning Method for Estimating Biomass of Grass Swards Using a Photogrammetric Canopy Height Model, Images and Vegetation Indices Captured by a Drone. Agriculture 8, 70. https://doi.org/10.3390/agriculture8050070

Vrieling, A., Fava, F., Leitner, S., Merbold, L., Cheng, Y., Nakalema, T., Groen, T., Butterbach-Bahl, K., 2022. Identification of temporary livestock enclosures in Kenya from multi-temporal PlanetScope imagery. Remote Sens. Environ. 279, 113110. https://doi.org/10.1016/j.rse.2022.113110

Waudby, H.P., Petit, S., Robinson, G., 2013. Pastoralists' knowledge of plant palatability and grazing indicators in an arid region of South Australia. Rangel. J. 35, 445–454. https://doi.org/10.1071/RJ13021

Welti, E.A.R., Kuczynski, L., Marske, K.A., Sanders, N.J., de Beurs, K.M., Kaspari, M., 2020. Salty, mild, and low plant biomass grasslands increase top-heaviness of invertebrate trophic pyramids. Glob. Ecol. Biogeogr. 29, 1474–1485. https://doi.org/10.1111/geb.13119

World Bank, 2018. Rural population (% of total population). World Bank.

Xue, J., Su, B., 2017. Significant Remote Sensing Vegetation Indices: A Review of Developments and Applications. J. Sens. 2017, e1353691. https://doi.org/10.1155/2017/1353691

Zach, 2021. Logarithmic Regression in R (Step-by-Step). Statology. URL https://www.statology.org/logarithmic-regression-in-r/ (accessed 2.10.24).

Zhang, Y., Fu, B., Sun, X., Yao, H., Zhang, S., Wu, Y., Kuang, H., Deng, T., 2023. Effects of Multi-Growth Periods UAV Images on Classifying Karst Wetland Vegetation Communities Using Object-Based Optimization Stacking Algorithm. Remote Sens. 15, 4003. https://doi.org/10.3390/rs15164003

Zhou, R., Yang, C., Li, E., Cai, X., Wang, X., 2023. Aboveground biomass estimation of wetland vegetation at the species level using unoccupied aerial vehicle RGB imagery. Front. Plant Sci. 14.

© University of Venda